

We are very grateful for the constructive comments and valuable suggestions offered by the three reviewers. The reviewers' comments appear in **bold** followed by our responses to each comment in *italics*. Line numbers in our responses refer to the edited manuscript.

Reviewer #1

General:

1. While I appreciate that NO-NO2 cycling is rapid, non-linear and highly complex, I would like to authors to be explicit in precisely which molecule they are considering the dry deposition of. They rather inconsistently refer to deposition of NO2 and of NOx. Presumably they are assuming that NO deposition is negligible and hence deposition of NO2 can be used as a proxy of NOx deposition. If so, this should be explicitly stated early in the manuscript and a single term used from that point on.

We have gone through the manuscript and have corrected mention of “NO_x deposition” to explicitly refer to “NO₂ deposition”. We also do use NO₂ as a proxy of NO_x deposition. A statement was added to P3, L26, clarifying that we consider NO deposition to be negligible.

Deleted: 17

2. The study purports to use two field sites, Blodgett Forest (BEARPEX campaign 2009) and University of Michigan Biological Station (UMBS campaign 2012). However, the authors almost exclusively focus their model description, parameterizations, sensitivity tests, results and discussions on Blodgett with scant details given to the results from UMBS other than to corroborate (or highlight differences) those from Blodgett. The authors should either reduce their analysis to a single site or, preferably, give similar attention to UMBS. The differences between model outcomes for the two sites is, to my mind, of real importance to enable the modelling and measurements communities to understand the processes that require further elucidation.

We have considered the reviewers comment. We believe similar giving similar attention to UMBS would distract from our focus on the conceptual conclusions of this paper. The purpose of including the UMBS data is to further corroborate the ideas in the model and to demonstrate that the model is applicable to multiple sites and not simply tuned for Blodgett Forest observations. The overall purpose of this manuscript is not to argue that observations should exactly match our model predictions, but rather to illustrate trends and key ideas that field observations and modelling studies should pay further attention to in future observational and modelling research. We added to P12, L4: “Similar trends (not shown) were also observed using parameters for UMBS.”

Deleted: 1

Deleted: 30

We also chose to focus our attention on Blodgett Forest for comparing the Wesely and Emberson models because this is a region subject to frequent dry conditions in the summer and fall, and view this site as an example of a region where our findings may be of particular importance.

3. While the authors explicitly quantify the differences in NOx concentrations and fluxes between the two deposition schemes and between the perturbed parameter sensitivity tests, they do not similarly evaluate the relative performances against observations, relying instead on qualitative, descriptive differences. The results would be far stronger if this aspect of the model outcome were better explored and presented.

We agree with the reviewer that it will be important in the future to directly and quantitatively compare models to observations. However, at this point in time, we believe clarifying key variables that govern NOx fluxes is an important advance even without such a quantitative comparison. Moreover, we are not aware of observations for a location during both dry and wet conditions. We call for more long-term observations of stomatal behaviour and dry deposition processes over a variety of meteorological conditions.

Specific:

Introduction

Throughout: All of the deposition models and studies presented here are specifically focused on the dry deposition of O3. The authors need to build a stronger argument that NO2 deposition should be assumed to follow the same process. In particular, in the case of O3, there still remain questions around the relative contributions of stomatal vs cuticular fluxes to the total leaf conductance. Most O3 deposition calculations assume that mesophyllic conductance is zero, is there evidence that this is the case for NO2.

We added a statement to ~~P3, L1-2~~ with citations arguing NO2 deposition is also controlled by stomatal opening. Mesophyllic resistance in models is indeed assumed to be comparatively small. However, this is a question we are actively researching with laboratory chamber measurements. This will be followed up in a future publication currently in preparation.

p2, L19 (and elsewhere): VPD is a convenient proxy for leaf water potential as it can be calculated from routinely measured meteorological variables but it is often not a good metric to use under conditions of drought.

We agree with the reviewer comment. However, the focus that we take on VPD is indeed because it is a convenient proxy that we believe is practical. Consideration of VPD is a substantial improvement over current CTMs that do not include such a parameterization. We note that this does not completely tell the whole picture, which we discuss later P13, ~~L23, P14, L2~~

p2, L20: make clear that “season” and “seasonality” refers to plant phenology

“season” was changed to “seasonality of leaf phenology”.

p3, L4-5 (and elsewhere): Technically, the DO3SE model estimates stomatal conductance for use in deposition schemes to calculate deposition velocities and hence O3 fluxes.

Line was changed to “...estimating stomatal conductance to predict ozone deposition velocities,...”

p3, L12: Could the authors explicitly state some of these “other molecules”

P3, ~~L28-30~~ now reads: “... other molecules such as NO2, NO, H2O2, HNO3, hydroxy nitrates, alkyl nitrates, peroxyacyl nitrates, etc....”

p3, L15-17: YES!!! This should be emphasised!

We agree, but are unsure what more we could do to emphasize this point.

2 Model description

p3, L21: A value of 100m for the PBL height during the peak growth season (summer) seems low, particularly for Blodgett. Under clear skies and high insolation I would expect to see values of 1500-2000m. Is their value based on observations at the two sites? If so, please provide references; if not please justify.

References to Wolfe and Thornton, (2011) and Wolfe et al., (2011) were added to ~~P4, L3~~

p3, 21: “Gaussian”

fixed

p3, L30: Δh is surely the height / depth of the box. I assume that the model has a horizontal scale of 1m2 or 1cm2, but please clarify this.

Deleted: P2

Deleted: L27

Deleted: 29

Deleted: 19

Deleted: 31

Deleted: , now P3, L5-6

Deleted: L19

Deleted: 2

Deleted: 3

Deleted: 29

Each box layer is treated as well-mixed and homogenous.

p4, L1-19: This paragraph (which should really be split in two for BEARPEX and UMBS) is not a description of the model, rather the two field sites and should have a separate section.

The paragraphs describing the two sites were separated into two paragraphs and a separate section added (2.2, P5, ~~L24~~–P6, L1~~8~~).

p4, L7: I am surprised that UMBS was modelled here without a separate understory, see e.g. Bryan et al (2015) Atmos Environ.

There is a separate understory. This has been clarified in P6, L~~6~~ and Table 1. Citation to Bryan et al., 2015 was also added.

p4, L20-21: Make clear here that this is simply following Beer's Law.

"...following Beer's law:" was added to P6, L~~15~~.

p4, L30: What are tau and TL in this context?

Please see Wolfe and Thornton, (2011). We added an additional citation of this paper following P6, L26. A definition was also added to P6, L27 : "... defined as the ratio of the "time since emission" of a theoretical diffusing plume (τ) and the Lagrangian timescale (TL)..."

p4, L30 (and Table 1): Where is the value of u^* taken from and why is it a constant value?

We used for u^ the average daytime value reported by Wolfe and Thornton, (2011). The range of u^* during the BEARPEX-2009 campaign was ~ 0.1 – 0.8 . We decided to use the daytime average as a constant value, as for the most part we restricted our analysis to daytime results. We ran a scenario with our model in which u^* above the canopy varied based on a sinusoidal fit to average diurnal observations at Blodgett Forest, and observed negligible changes to the canopy fluxes and above-canopy NO_x mixing ratios. Based on this, and our sensitivity test to τ/TL , we decided to leave out this additional complication in our model so that it would be easily extendable to forests where observations of u^* are not readily available.*

p5, L15: Please explain why the rate constants require adjustable parameters to make them site-specific. Are the authors assuming segregation? recycling?

To P7, ~~L30~~ we added the statement: "kOH and kNO3 are effective values adjusted in the model based on site-specific VOC composition and observations of OH reactivity."

p5, L21: Where are the basal emission rates taken from? Are they average values for deciduous and evergreen mid-latitude forests, site-specific, dominant-species specific?

Citations of the emissions rates and other parameters were added as a table caption for Table 1.

p5, L22: Deposition should be described in a separate section. In fact, given it is the main focus of the study, it should be the first.

We have rearranged the manuscript so Deposition appears in its own section and first in the section 2.1.

Deleted: L17

Deleted: 2

Deleted: ¶

Formatted: English (United States)

Deleted: 5

Deleted: 28

Deleted: 9

Deleted: L23

p5, L26-p6, L5: This is the Baldocchi parameterisation of total resistance. Why have the authors not used the subsequent Gao et al (1993) update?

The Baldocchi parameterization of total resistance is used because our model has been built to scale up laboratory observations of leaf-level deposition to the canopy scale. A similar approach was taken for CAFE model development (Wolfe and Thornton, 2011), on which this simplified model was based. In our opinion, the Gao update adds complexity without changing the aspects that are key to the discussion here.

p6, L5-7: If all processes are correctly included and parameterized there should be no need to use a compensation point; this is merely a formulation that is used when the production and loss terms are not fully represented in a model.

We changed the sentence (P4, ~~L29-30~~) to say: “We do not allow for emission of NO or NO₂ from leaves, consistent with recent laboratory observations that have observed negligible compensation points for these molecules (Chaparro-Suarez et al., 2011; Breuninger et al., 2013; Delaria et al., 2018).”

p6, L13: The authors have not defined SR

A definition of SR has been added P5, ~~L9~~.

p6, L14: Eqn 12 is essentially the Jarvis (1976) parameterisation of stomatal conductance. It has been modified since, with additional adjustment factors. It forms the basis of the DO3SE model, but really the DO3SE model is about the damage and therefore incorporates an additional modifying factor fo3 to the Jarvis expression for gs.

The Emberson et al. (2000) paper we refer to does not include this fO₃ term. We added a citation of Jarvis et al. (1976) to P5, ~~L4~~.

p7, L6 & L8: VOC or BVOC?

BVOC. This has been updated p ~~8~~, ~~L3~~.

p7, L16: Please expand on how fluxes are calculated within this model.

Fluxes are calculated according to Eq. 14 (updated manuscript). We added a reference to Wolfe and Thornton (2011) P6, ~~L22~~, as the same method of calculating fluxes was used here. Reference to Eq. 14 was also added to P8, ~~L20~~.

p7, L17: How is the PAN formation / NOx removal incorporated? It is not clear if or how these processes are included in the authors’ considerations of chemical production and loss, lifetime calculations and OPE.

As shown in the Romer et al. reference, during the day at high temperatures, PAN is in steady state with NO_x and a constant PAN/NO_x ratio occurs. PANs role in these circumstances is to sequester NO_x in a different form. In this paper, we neglect the possibility of direct PAN deposition. Upon deposition of NO₂, PAN dissociates maintaining the fixed PAN/NO_x ratio set by the steady-state. At night, PAN is assumed to be a permanent sink of NO_x and not available to return to the NO_x pool when NO₂ is removed by deposition.

We have removed this discussion of night time chemistry/deposition as it is not important to the conclusions of the paper.

3 Sensitivity to parameterizations:

As previously noted, this section appears only to consider Blodgett Forest (unless all parameters were the same at both sites, which other parts of the manuscript suggest was not the case)

Deleted: L21

Deleted: 22

Deleted: L2

Deleted: 4

Deleted: L28

Deleted: 7

Deleted: 22

Deleted: 15

Deleted: 14

p7, L22-23: How were these values of total deposition velocity chosen?

We edited P8, L28 to read: “...based on values of gmax and gmin chosen for Blodgett forest (discussed above) and typical values for deposition velocity observed for a variety of species in the laboratory (Teklemariam and Sparks, 2006; Chaparro Suarez et al., 2011, Breuninger et al., 2013, Delaria et al., 2018). “

Deleted: 1-23

p8, L10: Why have the authors chosen a value of 2 for tau/TL; Wolfe and Thornton (2011) used a value of 4 for this site when developing the CAFE model.

In our simplified model, a value of 2 resulted in the residence time in the canopy most similar to what was observed at Blodgett Forest. The simplified model gave a different residence time with a value of 4 than in the CAFE model.

p8, L10: “resulting in a canopy residence time of 152s” at both sites? Or just Blodgett?

“...for Blodgett Forest...” has been added to P9, L19 for clarification. We have also added the applicable UMBS residence time.

Deleted: 1

p8, L22: Please explain why Rb and specifically lw has a larger impact on species with high rates of leaf deposition.

At higher deposition velocities, the stomatal resistance is lower and Rb makes a greater contribution to the total resistance. We expect small changes in Rb under these conditions to have a greater overall effect. We have added to P9, L31: “...where Rb makes a greater contribution to the total resistance.”

Deleted: 23

p9, L14: I realise this is taken from a previous study but it is not clear why UMBS should be modeled using parameters for a European beech species when it is dominated by aspen.

We agree with the reviewer that parameters for aspen would have been more appropriate. However, there is no available data we are aware of for the specific tree species found at UMBS. As the site also contains American beech trees, and other hardwood deciduous tree species, a European beech species was chosen as a “best guess” for how trees at UMBS would behave. We realize this is not ideal, and call for more studies of stomatal regulation of North American trees. We note that the resulting predictions are in plausible agreement with observations and that the parameters used are distinct from those at Blodgett Forest, serving our purpose of showing that the model parameters we identify as important are flexible enough to represent different ecosystems.

p9, L19-p10, L4: Please quantify the model-obs fit rather than providing simply a qualitative overview.

We added references to figures 3 and 4 where appropriate, as well as parentheticals describing quantitative differences to P10, L24; P11, L12.

Deleted: 18

Deleted: 6

p9, L25: Please explicitly state what is meant by NOx enhancement. I think it is the difference between in-canopy and above canopy concentrations. But these will differ between levels in the canopy and PBL

This has been clarified in P10, L32: “... ,relative to above-canopy mixing ratios, ...”. A definition has also been added to the caption for Figure 3.

Deleted: 16

p10, L6: Wesely

Fixed.

5 **p10, L26-28: How do these deposition velocities compare with observations? In L10, the authors state that values of 1.4, 0.77 and 1 are used in global models. Do the author have site-specific measurements on which they have based their choice of 0.3 and 1.4 as upper and lower bounds?**

An upper bound of 1.4 was chosen from the upper bound of the global model listed above. Our lower-bound estimate was 0.1 cm s⁻¹, but we believe 0.3 cm s⁻¹ is a more reasonable lower bound estimate based on chamber studies we have recently conducted. Quantitative data for 0.1 cm s⁻¹ was added P12, L3-4 for consistency.

10 **p11, L1: The authors are comparing 2 sites with a range of differences so I'm not sure they can claim "regional" differences. Surely it's more to do with different forest types, different soils, different meteorology, . . . Please could the authors be a little more specific.**

We have made edits for accuracy on P12, L 6-7. The manuscript now reads: "The relative importance of including parameterizations of VPD and SWP in the calculation of stomatal conductance and overall deposition velocity is expected to be regionally variable, along with regional variations in dominant tree species, soil types, and meteorology."

15 **P11, L2: I have a problem with the use of "wet" and "dry" in this context as deposition itself is referred to as wet or dry. Perhaps the authors can find an alternative way to describe wet and dry environments (I couldn't think of an obvious alternative I'm afraid)**

We have considered the reviewers point and understand how referring to conditions as "wet" and "dry" is less than ideal. However, we also were unable to come up with a more appropriate way of referring to these conditions.

20 **p11, L4-7: Do these values of SWP and RH match long-term observations?**

Citations have been added to P12, L14-16 for our choices of "wet" and "dry" conditions.

25 **p11, L20-25: It would be good to see a more considered discussion of the results and the reasons (i.e the processes) behind the similarities and differences between the sites.**

The current discussion serves our purpose of showing that the model is plausibly related to a second location. More detailed analysis of similarities and differences strikes us as more appropriate when more extensive observations of NOx fluxes are available at a location.

30 **p12, L6-7: Suggest the authors extend their view beyond the USA. Surely their findings are GLOBALLY applicable?**

We considered the reviewer's suggestion, but we decided to leave as-is. We do not feel that giving an example of a region with frequent droughts in the US implies our finding will not be applicable globally. Our intention was to give one such example of a type of environment that our findings may be important for.

35 **p12, L9: CLM includes a specific parameterization of stomatal conductance and is the land surface model for both regional and global models of chemistry-climate (see Lombardozzi et al, various). Models with a full land surface module already calculate stomatal conductance and plant physiology so have no need to incorporate either the Wesely or Emberson approaches for estimating gs.**

40 **p12, L21-22: Following on from the above point, this point about the relative simplicity of the Emberson approach should be made explicitly clear from the outset by the authors.**

50

Deleted: 1

Deleted: 29

Deleted: 30

Deleted: 2

Deleted: 3

Deleted: 9

Deleted: 2

We have added a line to the introduction to highlight the simplicity of the Emberson model. “We consider here both the Wesely model and the similarly simplistic approach of Emberson et al. (2000) that incorporates effects of VPD and SWP.” We have also added a reference to the CLM P13, L2~~9-31~~.

Deleted: 4

Deleted: 26

p13, L2: How is OPE defined? As molecule of O3 produced per “molecule” of NOx lost?

This definition is correct. Please see Eq. 26.

p13, L8: PBL

The suggested change has been made to P14, L20.

Deleted: 18

p13, L20-p14, L10: Parameterized for BEARPEX again?

All relevant parameterizations have been listed in this section. However, the values chosen for α , VOC reactivity and P_{HOx} were similar to conditions at BEARPEX-09. A clarification has been made in L~~5~~ of P1~~5~~.

Deleted: 17

Deleted: 4

p13, L26: Is PBL height fixed?

Yes, this section describes a simple box-model that does not evolve in time.

p14, L1 and L3: The plots of observed NOx concentrations for both sites suggest they are $\sim \leq 1$ ppb so why have the authors explored up to 100 ppb here?

In our view, the purpose of a mechanistic model is to permit prediction outside the range of observations and to identify circumstances where a process is uniquely important. In this section, we explore the role of deposition in near-urban forests where NO_x concentrations are significantly higher than the two forests we focus on as our test examples. We find that NO_x loss via stomatally controlled deposition is the primary loss mechanism in cities. To our knowledge that idea is not described previously in the literature, at least not with a tool that has the potential for incorporation into quantitative modelling.

6 Conclusions

p14, L25: missing closing parenthesis.

Fixed.

p14, L30-31: It’s also imperative to accurately measure gs in a way that reflects differences between leaf-level and canopy-scale gs.

We agree with the reviewer.

p14, L31-32: DO3SE is NOT a deposition model; it is a model of stomatal conductance that can be used in a deposition scheme so effectively it also uses the resistance in series approach.

The wording has been changed for accuracy on P16, L14.

Deleted: 9.

p15, L1-4: Why is this important? What does this miss? Do we know that is wrong?

The text in the conclusions and paper points to several items that are important, including a mechanistic explanation for CRF, explicit modelling of stomatal opening, and recognition of NO_x fluxes as a significant control over the NO_x lifetime in a range of different circumstances. We do not believe it would help the reader for us to be repetitive on these points at this place in the text.

p15, L8: think GLOBAL!

Locations outside the US have been references P16, ~~L21-22~~,

Deleted: 17

p15, L8-9: Please could the authors be more specific in their recommendations? Precisely what do they mean by explore? More measurements? More modeling? And specifically of what, when and where?

Deleted: 18

Deleted: ¶

We have added a sentence to the end of the concluding paragraph:

“... explored with observations of NO_x fluxes and concurrent models to confirm the role of deposition in a wider range of environs and more thoroughly vet the conceptual model proposed here.”

Figures and Tables

p24, Fig 1: I am surprised that the authors have chosen only to vary PBL for the top two layers in the active mixed layer. I would expect the lower 2 of these layers to similarly evolve over the course of the day but with lower amplitude.

We do not believe this additional complication would change the general themes presented here, although they would certainly change things in detail.

p24, Fig 1: Right-hand labels on plot say “remnant” and caption says “residual”. Would personally use the latter.

Fixed.

p25, Fig 2: Not sure that this figure (or Fig S9) add anything to the paper. The authors have given the lat-long coordinates for both sites so readers could look for them on a map and they do not refer more than in passing to the figure from the text.

Deleted: ¶

Deleted: ¶

It is our impression that other readers may appreciate having the maps. Particularly for observing the relative proximity to urban centers.

p26, Fig 3(d): Clarify what is meant by NO_x enhancement in this context.

This has been clarified in the figure caption. NO_x enhancement is defined as NO_x at each height – NO_x above the canopy.

p27, Fig 4: A panel showing a time series of NO_x would be helpful for direct comparison between the two sites.

Deleted: ¶

We prefer to only show the diurnal average and variance.

p32, Fig 9: PAN? Daylight hours or 24-hour average?

This figure shows an average of daylight hours. This has been clarified in the figure caption. PAN is included in NO_x, as it is in steady-state with NO_x during the day (Romer et al., 2016).

Reviewer #2

We have added additional legends to some of the figures. We have also gone through our figure captions and tried to be as clear as possible about symbol meanings and more detailed in our descriptions where applicable.

Reviewer #3

We thank reviewer #3 for pointing out some of the complexities in representing canopy exchange. Here we have focused on a fairly simple representation because a model of this complexity is comparable to those utilized in regional or global models. We intend to focus less on the quantitative agreement and emphasize the key conceptual advances. We argue that to correctly represent the degree of complexity in atmosphere-biosphere interactions the new ideas we present are needed.

With these ideas alone, we are able to reach some significant insight—especially that CRF's are not necessary. We do not intend to suggest that the ideas we present alone are adequate to describe canopy scale mixing. The parameterization used here is designed to simulate conditions in two forests. In response to reviewer #3, we have added the following text P7, L1-8.

Our model is a simple parameterization of turbulent processes and as such will only capture mean vertical diffusion. Other work (Collineau and Brunet, 1993a; Raupach et al., 1996; Brunet and Irvine, 2000; Thomas and Foken, 2007; Sörgel et al., 2011; Steiner et al., 2011) has shown that “near-field” effects of individual canopy elements and coherent turbulent structures can play an important role in canopy exchange. These more intricate processes are not captured explicitly by our simple model. Previous work (Gao et al., 1993; Makar et al., 1999; Stroud et al., 2005; Wolfe et al., 2011) have also utilized fairly simple representations of canopy exchange in local and regional models. As such, K-theory is likely sufficient to represent average vertical diffusion for the purposes of our study.

In response to the concerns presented by Reviewer #3, on page C3, we have added a more detailed description of the representation of mixing that we use in our model, along with specific citations of the works cited by Wolf and Thornton (2011) and Reviewer #3. We have added the following to the text P6, L28-32.

The details of the parameterization of turbulent diffusion fluxes is documented elsewhere (Wolfe and Thornton, 2011) and based on the works of Raupach (1989) and Makar et al. (1999). The height dependent friction velocity ($u(z)^*$) is attenuated from the above-canopy u^* according to Yi et al. (2008). Although Finnigan et al. (2015) identified flaws in this treatment, we believe it is sufficient for our focus on illustrating generalizable qualitative trends.

The following statement was added to P12, L33-P13, L3:

We recognize that the multibox model presented in this work is a simplified representation of physical processes, and as such is not likely to (and is not intended to) provide quantitative exactitude for the trends described above. However, we argue for the necessity of incorporating these conceptual advances for accurately representing canopy processes and predicting their effect on the NO_x cycle.

Specific comments:

P6 L4: “and are dependent upon plant physiology.” => They also depend on the physical and chemical properties of the compounds.

On page 4, L26-27, (originally P6, L4), we have included the statement: “Rleaf is dependent upon plant physiology and the chemical and physical properties of the deposition compounds”.

Deleted: 6

Deleted: L25

Deleted: 32

Deleted: 20

Deleted: 24

Deleted: 0

Deleted: 33

Deleted: 19

Deleted: 20

P8 L31: Did the different canopy shapes change the residence times or was this kept constant? Are canopy structure and LAI independent from the residence time in the model?

5 *The different canopy shapes did change the residence time. The residence time for UMBS was added to P9, L18.*

Deleted: 1

**P9 second paragraph:
Here again the question how much influence has the “advection correction” here?**

10 *Specifics for how advection was treated in the model was added to P7, L17-18 and P11, L15.*

Deleted: 0

Deleted: 1

Deleted: 9

**Technical comments:
P3 L21: “below the boundary layer” => replace by either “within the pbl” or “below pbl top”.**

15 *We changed this to “...within the planetary boundary layer (PBL)”.*

P8 L31: “is was” => is

Fixed

20 **Fig.3 and 4: Please use same spacing of time axis for all panels. Makes it easier to compare.**

Fixed

25 **Figure 3d): which time intervals are used for “morning” and “afternoon”?**

Interval definitions were added to the figure caption.

30 **Figure 4b): Move NO₂ label in graph as the subscript 2 is hidden within the data points.**

Fixed

Editor:

35 *Please see changes made to the introduction section.*

A model-based analysis of foliar NO_x deposition

Erin R. Delaria¹, Ronald C. Cohen^{1,2}

¹Department of Chemistry, University of California Berkeley, Berkeley, CA, USA

²Department of Earth and Planetary Science, University of California Berkeley, Berkeley, CA, USA

Correspondence to: Ronald C. Cohen (rccohen@berkeley.edu)

Abstract.

Foliar deposition of NO₂ removes a large fraction of the global soil-emitted NO_x. Understanding the mechanisms of NO_x foliar loss is important for constraining surface ozone, NO_x mixing ratios, and assessing the impacts of nitrogen inputs to ecosystems. We have constructed a 1D multi-box model with representations of chemistry and vertical transport to evaluate the impact of leaf-level processes on canopy-scale concentrations, lifetimes, and canopy fluxes of NO_x. Our model is able to closely replicate canopy fluxes and above-canopy NO_x daytime mixing ratios observed during two field campaigns, one in a western Sierra Nevada pine forest (BEARPEX-2009) and the other a northern Michigan mixed hardwood forest (UMBS-2012). We present a conceptual argument for the importance of NO₂ dry deposition and demonstrate that NO₂ deposition can provide a mechanistic explanation for the canopy reduction of NO_x. We show that foliar deposition can explain observations suggesting as much as ~60% of soil-emitted NO_x is removed within forest canopies. Stomatal conductances greater than 0.1 cm s⁻¹ result in modelled canopy reduction factors in the range of those used in global models, reconciling inferences of canopy NO_x reduction with leaf-level deposition processes. We show that incorporating parameterizations for vapor pressure deficit and soil water potential has a substantial impact on predicted NO₂ deposition in our model, with the percent of soil NO_x removed within one canopy increasing by ~15% in wet conditions compared to dry conditions. NO₂ foliar deposition was also found to have a significant impact on ozone and nitrogen budgets under both high and low NO_x conditions.

Deleted: Our model demonstrates

Deleted: factors (CRFs).

Deleted: also show

1 Introduction

The chemistry of nitrogen oxides (NO_x ≡ NO + NO₂) has a large impact on the oxidative capacity of the atmosphere and the budget of global surface ozone (Crutzen, 1979). NO_x is primarily removed from the atmosphere by chemical reactions to form nitric acid, alkyl nitrates, and peroxy nitrates, and by dry deposition of NO₂ (Crutzen, 1979; Jacob and Wofsy, 1990; Romer et al. 2016). The chemical loss pathways of NO_x have been extensively studied, but the physical loss of NO₂ to dry deposition remains much more uncertain. Globally, foliar deposition of NO₂ removes 20–50% of soil-emitted NO (Jacob and Wofsy, 1990; Yienger and Levy, 1995), and constrains near-surface NO_x concentrations and input to ecosystems (Hardacre et al. 2015). Understanding the processes that control this removal of NO_x by the biosphere is important for predicting anthropogenic surface ozone and understanding flows in the nitrogen cycle.

Reactive nitrogen oxides also serve as an important nutrient in ecosystems. Exchange processes cycle nitrogen between the biosphere and atmosphere, influencing the availability of nitrogen to ecosystems (Townsend et al., 1996; Holland

et al., 1997; Galloway et al., 2004; Holland et al., 2005). Deposition of atmospheric reactive nitrogen species can fertilize ecosystems with limited nitrogen availability (Ammann et al., 1995; Townsend et al., 1996; Williams et al., 1996; Holland et al., 1997; Galloway et al., 2004; Teklemariam and Sparks, 2006). Although nitrogen is often the limiting nutrient for plant growth (Oren et al., 2001; Galloway et al., 2004), anthropogenic activities have in some cases caused an excess loading of nitrogen to ecosystems, leading to dehydration, chlorosis, soil acidification, and a decline in productivity (Vitousek et al., 1997; Fenn et al., 1998; Galloway et al., 2004).

The current understanding of the exchange of nitrogen oxides between the atmosphere and biosphere remains incomplete. Despite the importance of dry deposition processes, they are among the most uncertain and poorly constrained aspects of atmosphere-biosphere nitrogen exchange and the tropospheric budgets of O_3 and NO_x (Wild, 2007; Min et al., 2014;

Hardacre et al., 2015). This uncertainty arises from the complex dependence of dry deposition processes on surface cover,

meteorology, seasonal changes in leaf area index (LAI), species of vegetation, and the chemical species carrying odd-N.

Developing a mechanistic understanding of dry deposition of NO_2 has largely depended on inferences from scarce long-term field observation data and a limited number of laboratory studies on the effects of environmental factors on deposition at the

leaf-level. This understanding is represented by a deposition velocity, V_d . Many global scale chemical transport models

(Wesely, 1989; Jacob and Wofsy, 1990; Ganzeveld and Lelieveld, 1995; Wang and Leuning, 1998; Ganzeveld et al., 2002a)

parameterize V_d using the resistance in-series approach similar to that developed by Baldocchi et al. (1987). These treatments

are heavily parameterized, leading to a large degree of uncertainty, many of which (Jacob and Wofsy, 1990; Wesely, 1989) do

not account for the effects of VPD, SWP, CO_2 mixing ratio, or other factors known to influence stomatal conductance

(Hardacre et al., 2015). A common approach for modelling canopy uptake of trace gases is with a one- or two- layer “big-leaf”

dry deposition model, in which the forest is treated as having a characteristic “average” deposition velocity (Hicks et al. 1987;

Wesely, 1989; Ganzeveld and Lelieveld 1995; Wang and Leuning, 1998; Zhang et al., 2002). However, Ganzeveld et al.

(2002a) implemented a multi-layer column model in a global chemistry and general circulation model GCM-ECHAM

(European Centre Hamburg Model) and demonstrated the importance of considering interactions within the canopy,

particularly in pristine forest sites. More comprehensive treatments of atmosphere-biosphere exchange are thus needed in

global models.

The deposition velocity of NO_2 to vegetation is largely regulated by stomatal conductance (Johansson, 1987; Thoene

et al., 1991; Rondon and Granat, 1994; Teklemariam and Sparks, 2006; Chaparro-Suarez et al., 2011; Breuninger et al., 2012;

Delaria et al., 2018), which varies with tree species, photosynthetically active radiation (PAR), vapor pressure deficit (VPD),

temperature (T), soil water potential (SWP) and seasonality of leaf phenology (Emberson et al., 2000; Zhang et al., 2003;

Altimir et al., 2004; Hardacre et al., 2015; Kavassalis and Murphy, 2017). NO_2 deposition remains even more uncertain than

deposition of O_3 , where stomatal response has been shown to be the primary regulator of foliar deposition and mesophyll

resistance to deposition is negligible. Observations from leaf-level laboratory studies suggest the deposition of NO_2 is also

controlled by stomatal aperture (Hanson and Lindberg, 1991; Rondon and Granat, 1994; Hereid and Monson, 2001;

Teklemariam and Sparks, 2006; Pape et al., 2008; Chaparro-Suarez et al., 2011; Breuninger et al., 2012; Delaria et al., 2018),

Deleted: NO_x

Deleted: Many global scale chemical transport models (Jacob and Wofsy, 1990; Wang and Leuning, 1998; Ganzeveld et al., 2002a) parameterize V_d using the resistance in-series approach similar to that developed by Wesely (1989). These treatments are heavily parameterized, leading to a large degree of uncertainty, and do not account for the effects of VPD, SWP, CO_2 mixing ratio, or other factors known to influence stomatal conductance (Hardacre et al., 2015). NO

Deleted: NO_x

however, reactions in the mesophyll may also be important for controlling the deposition velocity of NO₂ (Teklemariam and Sparks, 2006; Breuninger et al., 2012). A failure to consider the effects of relevant meteorology on stomatal conductance, as well as our deficient understanding of mesophyll resistances and the diversity of ecosystem responses, severely limits our ability to understand dry-deposition processes and how they will be affected by feedbacks from changes in climate, land use, and air pollution.

The importance of these considerations has recently been illustrated by Kavassalis and Murphy (2017), who found a significant correlation between VPD and ozone loss, and demonstrated that modeling using VPD-dependent parameterizations of deposition better predicted the correlation they observed. Previous work by Altimir et al. (2004) and Gunderson et al. (2002) have described the effects of VPD and other environmental parameters on the stomatal conductance to O₃ of *Pinus sylvestris* and *Liquidambar styraciflua*, respectively. More recent models, like the DO3SE model for estimating stomatal conductance to predict ozone deposition velocities, fluxes and damage to plants, incorporate the effects of VPD and SWP on stomatal conductance. No similar model exists for assessing these effects on NO_x deposition, although Ganzeveld et al. (2002b) included the effect of soil moisture availability for evaluating the role of canopy NO_x uptake on canopy NO_x fluxes. The DO3SE has successfully been implemented in the European Monitoring and Evaluation Program (EMEP) regional model (2012). Modelling studies by Buker et al. (2007) and Emberson et al. (2000) have also demonstrated the success of regional-scale parameterizations using observed relationships between meteorology and stomatal conductance for application to O₃. Such treatments of VPD and SWP were incorporated into a regional air quality model by Zhang et al. (2002 and 2003).

In this study we present a simplified multi-layer atmosphere-biosphere exchange model and investigate the sensitivity of NO_x canopy fluxes, ozone production, NO_x vertical profiles, and NO_x lifetimes to different parameterizations of stomatal conductance and deposition velocity. We consider here both the Wesely model and the similarly simplistic approach of Emberson et al. (2000) that incorporates effects of VPD and SWP. We restrict our considerations to the effects of different stomatal resistance parameterizations on predicted deposition velocities, as the magnitude of the mesophyll resistance remains uncertain and is assumed to be comparatively small in atmospheric models (Zhang et al., 2002). We also restrict our considerations to NO₂ deposition, as NO deposition has been shown to be negligible in comparison (Delaria et al., 2018). There have been many studies investigating the effects of dry-deposition parameterizations on deposition velocities—particularly of ozone—and the abilities of different modeling schemes to reproduce observational data for other molecules such as NO₂, NO, H₂O₂, HNO₃, hydroxy nitrates, alkyl nitrates, peroxyacyl nitrates, etc. (Zhang et al., 1996; Wang et al., 1998b; Emberson et al., 2000; Ganzeveld 2002; Buker et al., 2007; Wolfe et al., 2011; Hardacre et al., 2015; Nguyen et al., 2015). However, there has been little evaluation of how changes in dry deposition of NO₂ may affect surface mixing ratios and chemistry of important atmospheric species. Assessing the sensitivity to NO₂ deposition is crucial not only for evaluating the potential impact of uncertainties in dry-deposition parameterizations for global and regional models, but for understanding how a changing climate may influence NO_x, surface ozone, and the nitrogen cycle.

Deleted: mesophyll resistance

Deleted: is

Deleted: Chaparro-Suarez et al., 2011

Deleted: ozone

Deleted: , but n

Deleted: .

Deleted: , leaf area index, and deposition velocity

Deleted:

Deleted: Wang and Leuning, 1998;

Deleted: the

Deleted: of

2 Model description

We have constructed a simple atmospheric model for investigating the influence of leaf-level NO₂ foliar deposition on canopy scale NO_x lifetimes and concentrations. The model consists of eight vertical boxes within the planetary boundary layer (PBL), taken to be 1000 m during the day and 60 m at night (Wolfe and Thornton, 2011; Wolfe et al., 2011). The increase in PBL height during the day is treated as a Gaussian function of time with 98% of the integrated area contained between sunrise and sunset, with the maximum height reached at the time of maximum daily temperature (Fig.1).

In each box, the change in concentration (C) of species i, is calculated using the time-dependent continuity equation:

∂Ci(z)/∂t = P(z) + L(z) + E(z) + D(z) + A(z) + ∂F(z)/∂z (1)

where the terms on the right are the chemical production, chemical loss, emission, deposition, advection, and turbulent flux, respectively. In each box (k=1–8) the altitude (z) is considered as the average of the altitudes at the upper boundaries of boxes k and k – 1 (the midpoint of box k). The change in concentration for species i is calculated for each time step Δt = 2 s (Table 1).

ΔCi,k = (Pi,k + Li,k + Ei,k + Di,k + Ai,k + Fi,k/Δhk) Δt (2)

where Δhk is the width of box k. The only species not treated in this manner is the hydroxyl radical (OH), which is calculated using a steady-state approximation.

2.1 Deposition

The deposition flux (Fdep) of each depositing species i in the canopy is calculated according to:

Fdep = -Vd · LAI · Ci (3)

where LAI is the leaf area index, and Vd is the deposition velocity. The deposition velocities are calculated according to:

Vd = 1/R (4)

where R is the total resistance to deposition.

Rleaf = (1/Rcut + 1/(Rst+Rm))^-1 (5)

R = Ra + Rb + Rleaf (6)

where Ra, Rb, Rcut, Rst, and Rm are the aerodynamic, boundary layer, cuticular, stomatal, and mesophilic resistances, respectively. These resistances describe the turbulent transport of a gas to the surface (Ra), molecular transport through a thin layer of air above the leaf surface (Rb), and deposition to the leaf surface (Rleaf) (Baldocchi et al., 1987). Rleaf is dependent upon plant physiology and the chemical and physical properties of the deposition compounds. Rleaf is determined by deposition to the leaf cuticles (Rcut), diffusion through the stomata (Rst), and chemical processing within the mesophyll (Rm). We do not allow for emission of NO or NO2 from leaves, consistent with recent laboratory observations that have observed negligible compensation points for these molecules (Chaparro-Suarez et al., 2011; Breuninger et al., 2013; Delaria et al., 2018).

Deleted: detailed

Deleted: NOx

Deleted: below

Deleted: g

Deleted: 7

Deleted: 8

Deleted: 9

Deleted: 10

Deleted: and

Deleted: include compensation points in our parameterization NOx dry deposition

Deleted: in accordance

Deleted: numerous

Deleted: studies

Deleted: no evidence of NO2 emission at low NOx mixing ratio

All boundary, aerodynamic, cuticular, and soil resistances of O_3 , HNO_3 , CH_2O , alkyl nitrates (ANs) and acylperoxy nitrates (APNs), $HC(O)OH$, $ROOH$, and H_2O_2 are calculated according to Wolfe et al. (2011). The cuticular and mesophyll resistances for NO_2 and NO are adjustable input parameters. Stomatal resistances are determined from the stomatal conductance to water vapor (g_s) calculated using either Eq. 7 (Wesely, 1989), or Eq. 8 (Jarvis et al., 1976; Emberson et al., 2000), hereafter referred to as the Wesely and Emberson schemes, respectively:

$$g_s = g_{max} \times \frac{T(40-T)/400}{(1+(200(SR+0.1)^{-1})^2)} \quad (7)$$

$$g_s = g_{max} \times f_{phen} \times f_{light} \max \{f_{min}, (f_{temp} \times f_{VPD} \times f_{SWP})\} \quad (8)$$

where g_{max} is the species-specific maximum stomatal conductance, f_{min} is a species-specific scaling factor to the minimum stomatal conductance, SR is the solar radiation in $W\ m^{-2}$, and f_{phen} , f_{SWP} , f_{light} , f_{temp} , and f_{VPD} are functions representing modifications to the stomatal conductance due to leaf phenology, soil water content, irradiance, temperature, and vapor pressure deficit, respectively (Eq 9-12).

$$f_{light} = 1 - \exp(-Light_a \times PPFD) \quad (9)$$

$$f_{temp} = 1 - \frac{(T - T_{opt})^2}{(T_{opt} - T_{min})^2} \quad (10)$$

$$f_{VPD} = \min \left\{ 1, \left((1 - f_{min}) \times \frac{(VPD_{min} - VPD)}{(VPD_{min} - VPD_{max})} \right) + f_{min} \right\} \quad (11)$$

$$f_{SWP} = \min \left\{ 1, \left((1 - f_{min}) \times \frac{(SWP_{min} - SWP)}{(SWP_{min} - SWP_{max})} \right) + f_{min} \right\} \quad (12)$$

T_{opt} and T_{min} are the optimal and minimum temperature required for stomatal opening. PPFD is the photosynthetic photon flux density and $Light_a$ is a species-specific light response parameter. VPD_{min} and VPD_{max} are the vapor pressure deficit at which stomatal opening reaches a minimum and maximum, respectively. SWP_{min} and SWP_{max} are the soil water potentials at which stomatal opening reaches a minimum and maximum, respectively. All model calculations represented the peak growing season when $f_{phen} = 1$. f_{temp} , f_{VPD} , and f_{light} were calculated according to Emberson et al. (2000) using parameters found in Table 2.

2.2 Site description

The model was evaluated with comparison to observations from the Biosphere Effects on Aerosols and Photochemistry 2009 (BEARPEX-2009) field campaign from 15 June – 31 July 2009 at Blodgett forest (Min et al., 2014), and the University of Michigan Biological Station (UMBS) during 5 August – 10 August 2012 (Geddes and Murphy, 2014). For the BEARPEX-2009 calculations, the modelled canopy included an overstory height of 10 m with a one-sided leaf area index (LAI) of $3.2\ m^2\ m^{-2}$ (LAI_{os}), and an understory height of 2 m with a LAI of $1.9\ m^2\ m^{-2}$ (LAI_{us}). Model simulations were run for June 30, 2009 using conditions from the BEARPEX-2009 ponderosa pine forest site located in the western foothills of the

Deleted: 11

Deleted: 12

Deleted: 11

Deleted: 12

Deleted: 13

Deleted: 6

Deleted: 13

Deleted: 4

Deleted: 5

Deleted: 6

Formatted: Tab stops: 6.99", Right + Not at 6.14"

Deleted: is

Deleted: by

Sierra Nevada Mountains, CA (38°58'42.9"N, 120°57'57.9"W, elevation 1315 m) (Table 1) (Fig. 2a). Meteorological conditions and soil NO_x emissions used in the model simulation were those reported by Min et al. (2014). Diurnal soil water potentials (SWP) were values reported in a geological survey of nearby Sierra sites in a comparatively wet year (Ishikawa and Bledsoe, 2000; Stern et al., 2018).

For UMBS-2012 calculations, the modelled canopy included an overstory height of 20 m with a one-sided LAI of 2.5 m²m⁻², and an understory height of 4 m with a LAI of 1 m²m⁻² (Bryan et al. 2015). Model simulations were run for August 8, 2012 using conditions from the UMBS mixed hardwood forest located in northern Michigan (45°33'32" N, 84°42'52" W) (Table 1) (Fig 2b). Daily temperatures, VPDs, soil NO_x emissions and site-specific parameters used in the model simulations were those reported in Geddes and Murphy (2014), and Seok et al. (2013).

Temperature and relative humidity used in the model were sinusoidal fits to observations of minimum and maximum daily temperature and relative humidity from the corresponding field measurement site. The relative temperature decrease as a function of altitude was calculated using a fit to observations during BEARPEX-2007, as presented by Wolfe and Thornton (2011). Solar zenith angles (SZA) and photosynthetically active radiation (PAR) were calculated every 0.5 h for each location and time period using the National Center for Atmospheric Research TUV calculator (Madronich and Flocke, 1999) and fit using a smoothed spline interpolation. Within the canopy, extinction of radiation (ER) was calculated following Beer's law:

$$ER_k = \exp\left(-\frac{k_{rad}LAI_{cum}}{\cos(SZA)}\right) \quad (13)$$

where k_{rad} is the radiation extinction coefficient, SZA is the solar zenith angle, and LAI_{cum} is the cumulative LAI calculated as the sum of one-half the LAI in box k and the total LAI in the boxes above box k .

2.3 Vertical transport and advection

The turbulent diffusion flux ($F(z)$) is represented in the model using K-theory, according to the Chemistry of Atmosphere-Forest Exchange (CAFE) Model (Wolfe and Thornton, 2011).

$$F(z) = -K(z) \frac{\Delta C_{i,k}}{\Delta z} \quad (14)$$

where $\Delta C_{i,k}$ is the change of concentration in species i in box k during each timestep and Δz is the difference between the midpoints of boxes k and $k + 1$. $K(z)$ above the canopy is based on the values from Gao et al. (1993) and below is a function of friction velocity calculated according to Wolfe et al. (2011) and is a function of the diffusion timescale ratio (τ/T_L)—defined as the ratio of the “time since emission” of a theoretical diffusing plume (τ) and the Lagrangian timescale (T_L)—and the friction velocity (u^*) (Wolfe and Thornton, 2011). The details of the parameterization of turbulent diffusion fluxes is documented elsewhere (Wolfe and Thornton, 2011) and based on the works of Raupach (1989) and Makar et al. (1999). The height dependent friction velocity ($u(z)^*$) is attenuated from the above-canopy u^* according to Yi et al. (2008). Although Finnigan et al. (2015) identified flaws in this treatment, we believe it is sufficient for our focus on illustrating generalizable qualitative trends.

Deleted: x

Deleted: total

Deleted: 3

Deleted: .

Deleted: In the BEARPEX-2009 case, meteorological conditions and soil NO_x emissions used in the model simulation were those reported in Min et al. (2014). Diurnal soil water potentials (SWP) were values reported in a geological survey of nearby Sierra sites and a comparatively wet year (Ishikawa and Bledsoe, 2000; Stern et al., 2018). For the UMBS-2012 case, d

Deleted: x

Deleted: as

Deleted: 1

Deleted: T

Deleted: :

Deleted:

Deleted:

Deleted:

Deleted: and

The resulting residence time in the canopy is approximately 2–3 min for model conditions during the day. Our model is a simple parameterization of turbulent processes and as such will only capture mean vertical diffusion. Other works (Collineau and Brunet, 1993a; Raupach et al., 1996; Brunet and Irvine, 2000; Thomas and Foken, 2007; Sörgel et al., 2011; Steiner et al., 2011) have shown that “near-field” effects of individual canopy elements and coherent turbulent structures can play an important role in canopy exchange. These more intricate processes are not captured explicitly by our simple model. Previous work (Gao et al., 1993; Makar et al., 1999; Stroud et al., 2005; Wolfe et al., 2011) have also utilized fairly simple representations of canopy exchange in local and regional models, and as such K-theory is likely sufficient to represent average vertical diffusion for the purposes of our study.

Advection in the model is treated as a simple mixing process in each model layer.

$$\left(\frac{dC_i}{dt}\right) = -k_{mix}(C_i - C_{i(adv)}) \quad (15)$$

where $k_{mix} = 0.3 \text{ h}^{-1}$ (Wolfe and Thornton, 2011), and $C_{i(adv)}$ is the advection concentration of species i . Advection concentrations are set to fit with the observations during BEARPEX-2009 (Min et al., 2014) or UMBS-2012 (Geddes and Murphy, 2014; Seok et al., 2013) and are used to maintain reasonable background concentrations (Table S1). Concentrations of NO_x , O_3 , and some VOCs at both sites were influenced by emissions from nearby cities and consequently had sources outside the canopy. For the BEARPEX-2009 model runs, the maximum daily advection concentration was reached at around 17 hrs, based on field observations of higher NO_x plumes from near-by Sacramento in the afternoon (Wolfe et al., 2011; Min et al., 2014). The diurnal advection concentrations of NO_x were fit to a Gaussian in the range 0.1–0.35 ppb (Table S1). For UMBS all advection concentrations were constant.

2.4 Chemistry

Chemistry in the model is based on reaction rate constants from the JPL Chemical Kinetics and Photochemical Data Evaluation No. 18 (Burkholder et al., 2015). Photolysis rates are calculated as a function of solar zenith angle (SZA), which was constructed using a smoothed spline interpolation fit of photolysis rates calculated with the TUV calculator (Madronich and Flocke, 1999) at every ten-degree interval of the zenith angle. The simplified reaction scheme included in the model is based on the model presented in Browne and Cohen (2012). The model includes both daytime and night-time NO_x chemistry and a simplified oxidation scheme. In this simplified case, oxidation of volatile organic compounds (VOCs) during the daytime results in the production of peroxy radicals (RO_2), treated as a uniform chemical family. To be applicable to a range of forest types, we also include adjustable parameters, k_{OH} and k_{NO_3} for the average rate constant for reaction of VOC with OH and NO_3 , respectively. k_{OH} and k_{NO_3} are effective values adjusted in the model based on site-specific VOC composition and observations of OH reactivity. A complete list of reactions and rate constants included in the model is shown in Table S2.

Deleted: s

Deleted:

Deleted: given in

Deleted:

Deleted: 2

Deleted: site-specific

Deleted: .

2.5 BVOC emissions

Emissions rates (molecules cm⁻³s⁻¹) of biogenic volatile organic compounds (BVOCs) in the canopy are calculated via:

$$E(z) = \frac{E_b}{\Delta h} C_L(z) C_T(z) LAI \quad (16)$$

where E_b (molecules cm(leaf)⁻² s⁻¹) is the basal emission rate of VOC, Δh is the total height of the box, and C_L and C_T are corrections for light and temperature (Guenther et al., 1995).

2.6 Evaluation of NO_x fluxes and lifetimes

The model was used to assess the impact of NO₂ deposition parameters on the NO_x budget, lifetime, loss, and vertical profile within a forested environment. In each box, the rates of NO_x loss with respect to nitric acid formation, alkyl nitrate formation, and deposition were calculated from Eq. 17–19.

$$L_{NO_x \rightarrow HNO_3} = k_{OH+NO_2}[OH][NO_2] + k_{N_2O_5 \text{ hydrolysis}}[N_2O_5] + k_{NO_3+aldehyde}[\text{aldehyde}][NO_3] \quad (17)$$

$$L_{NO_x \rightarrow RONO_2} = \alpha k_{NO+RO_2}[NO][RO_2] + \beta k_{NO_3}[NO_3][BVOC] \quad (18)$$

$$L_{NO_x \rightarrow Dep} = F_{dep}/\Delta h_k \quad (19)$$

α is the fraction of the NO + RO₂ reaction that forms alkyl nitrates and β is the fraction of the NO₃ + BVOC reaction that forms alkyl nitrates. The NO_x lifetime was then scaled to the entire boundary layer by summing over the products of the lifetime and boundary layer fraction ($\Delta h_k/PBL$) in each box

$$\tau_{PBL} = \frac{\sum_{k=1}^8 [NO_x]_k}{\sum_{k=1}^8 (L_{NO_x \rightarrow Dep} + L_{NO_x \rightarrow RONO_2} + L_{NO_x \rightarrow HNO_3})} \quad (20)$$

NO_x was treated as the sum of NO, NO₂, and all short-lived products, including NO₃, 2N₂O₅, and peroxyacetyl nitrate (PAN) (Romer et al., 2016). Deposition of PAN was not considered.

We also calculated the 24 h average vertical fluxes (Eq. 14) of NO_x, and used the flux through the canopy to estimate the fraction of soil emitted NO_x ventilated to the troposphere above. Because PAN formed during the nighttime is expected to re-release NO_x to the atmosphere during the day, in this calculation, PAN was included as part of the NO_x budget.

3 Sensitivity to parameterizations

We assessed the sensitivity of the model to τ/T_L , the radiation extinction coefficient (k_{rad}), the aerodynamic leaf width (l_w), LAI, soil NO emission (eNO), and α . These parameters are simplifications of complex physical processes and not always easily constrained by observations. The total deposition velocity of NO₂ chosen for these assessments was 0.2 cm s⁻¹ during the daytime and 0.02 cm s⁻¹ during the nighttime, based on values of g_{max} and g_{min} chosen for Blodgett forest (discussed above) and typical values for deposition velocity observed for a variety of species in the laboratory (Teklemariam and Sparks, 2006; Chaparro Suarez et al., 2011, Breuninger et al., 2013, Delaria et al., 2018).

Deleted: 3

Deleted: E

Deleted: and deposition

Deleted:

Deleted: The deposition flux (F_{dep}) of each depositing species the canopy is calculated according to:

$$F_{dep} = -V_d \cdot LAI \cdot C_i \quad (7)$$

where LAI is the leaf area index, and V_d is the deposition velocity. The deposition velocities are calculated according to:

$$V_d = \frac{1}{R} \quad (8)$$

where R is the total resistance to deposition.

$$R_{leaf} = \left(\frac{1}{R_{cut}} + \frac{1}{R_{st} + R_m} \right)^{-1} \quad (9)$$

$$R = R_a + R_b + R_{leaf} \quad (10)$$

where R_a , R_b , R_{cut} , R_{st} , and R_m are the aerodynamic, boundary layer, cuticular, stomatal, and mesophilic resistances, respectively. These resistances describe the turbulent transport of a gas to the surface (R_a), molecular transport of through a thin layer of air at the leaf surface (R_b), and deposition to the leaf surface (R_{leaf}) (Baldocchi et al., 1987). R_{leaf} is dependent upon plant physiology and determined by deposition to the leaf cuticles (R_{cut}), diffusion through the stomata (R_{st}), and chemical processing within the mesophyll (R_m). We do not include compensation points in our parameterization of NO_x dry deposition, in accordance with numerous recent studies that have observed no evidence of NO₂ emission at low NO_x mixing ratios (Chaparro-Suarez et al., 2011 Breuninger et al., 2013; Delaria et al., 2018).

All boundary, aerodynamic, cuticular, and soil resistances of O₃, HNO₃, CH₂O, alkyl nitrates (ANs) and peroxyacetyl nitrates (APN) HC(O)OH, ROOH, and H₂O₂ are calculated according to Wolfe et al. (2011). The cuticular and mesophilic resistances for NO₂ and are adjustable input parameters. Stomatal resistances are determined from the stomatal conductance to water vapor (g_s) calculated using either Eq. 11 (Wesely, 1989), or Eq. 12 (Emberson et al., 2000), hereafter referred to as the Wesely and Emberson schemes, respectively:

$$g_s = g_{max} \times \frac{T(40-T)/400}{(1+200(SR+0.1)^{-1})^2} \quad (11)$$

Deleted: 4

Deleted: NO_x

Deleted: s

Deleted: s

Deleted: , during the daytime,

Deleted: . During the nighttime PAN has a longer atmospheric lifetime (>10 h) and was treated as a permanent sink

Deleted: Lifetime against PAN formation at night was calculated from:

Deleted:

Deleted: NO_x

Deleted: -

Deleted: ;

Deleted: .

The largest effects were observed for changes in α , LAI, and soil NO emission. LAI_{os} and LAI_{us} were scaled from their values of 1.9 m²/m² and 3.2 m²/m², respectively by a factor of 0.25 and 1.5. Increasing the scaling factor from 0.25 to 1.5 resulted in a decrease of NO_x lifetimes, above canopy concentration, and average canopy flux of 24%, 27%, and 36%, respectively (Fig. S1). Increasing α from 0.01 to 0.1 resulted in a decrease in NO_x lifetimes, above canopy concentrations, and average canopy fluxes of 75%, 38%, and 39%, respectively (Fig. S2). For all other model runs an α of 0.075 was chosen, in accordance with observations from regions primarily influenced by BVOCs (eg. monoterpenes, isoprene, 2-methyl-3-buten-2-ol). Increasing the maximum soil NO emission from 1 to 10 ppt m s⁻¹ increased the in-canopy enhancement from 28% to 140% relative to above-canopy NO_x concentrations (Fig. S3b). The fraction of soil-emitted NO_x ventilated through the canopy also increased from 45% to 64% (Fig. S3a). The large effect of soil NO emission on NO_x fluxes implies that this highly variable parameter (Vinken et al., 2014) is also important to constrain in chemical transport models. Further discussion of soil NO emission is, however, beyond the scope of this study.

Very small effects on NO_x were observed for changes in the parameters τ/T_L , k_{rad} , or l_w . The minor changes caused by variations in these parameters are listed below for completeness:

τ/T_L represents the diffusion timescale ratio, a full description of which can be found in Wolfe and Thornton (2011).

Larger τ/T_L represents faster diffusion and vertical transport within the canopy layer, and shorter residence times in the canopy. We find that altering this parameter from 1.2 to 8 (representing a change in residence time from 650 s to 62 s) caused a 9.9%, 4.4%, and 8.7% increase in average canopy fluxes, NO_x lifetimes and above canopy concentration, respectively (Fig. S4). For all subsequent model runs, a value of 2 for τ/T_L was chosen, resulting in a canopy residence time during the day of 152 s and 194 s for Blodgett Forest and UMBS, respectively, calculated using Eq. 21.

$$\tau_{can} = h_{can} \sum_{k=1}^3 \frac{\Delta h_k}{K(z_k)} \quad (21)$$

The boundary layer resistance, or laminar sublayer resistance, R_b , is dependent upon the aerodynamic leaf width, l_w (Eq. 22)

$$R_b = \frac{cv}{Du^*(z)} \left(\frac{l_w u^*(z)}{v} \right)^{1/2} \quad (22)$$

where $v = 0.146$ cm²s⁻¹ is the kinematic viscosity of air, D is the species-dependent molecular diffusion coefficient, c is a tunable constant set to 1 for this study, and $u^*(z)$ is the height-dependent friction velocity that is a function of u^* and LAI_{cum} (Wolfe and Thornton, 2011). l_w depends upon the vegetation species. A value of 1 cm was chosen for the overstory and 2 cm for the understory, as these widths are characteristic of pine trees and understory shrubs in a poderosa pine forest (Wolfe and Thornton, 2011). Species with rapid deposition to the cuticles or the stomata are expected to be more sensitive to errors in l_w , such as HNO₃ or H₂O₂. An increase in NO_x lifetime, average canopy flux, and above canopy concentration of 1.4%, 2.4%, and 2.8%, respectively, was predicted for a change in l_w scaling factor from 0.1 to 2 (Fig. S5). These changes are expected to be greater in forests with a larger average deposition velocity, where R_b makes a greater contribution to the total resistance.

The rates of stomatal gas exchange and photolysis are regulated by the intensity of light that penetrates the canopy. The extinction of radiation by the canopy, treated as a Beer's Law parameterization (Eq. 113) is exponentially proportional to

Deleted: s

Deleted: s

Deleted: s

Deleted: ,

Deleted: 2

Deleted: 2

Deleted: This residence time is consistent with observations of variety of forest environments (Jacob and Wofsy, 1990; Wolfe et al. 2011).¶

Deleted: 3

Deleted: 3

Formatted: English (United States)

Deleted: e

Deleted: is

Formatted: Font: Italic

Formatted: English (United States)

Deleted: .

Deleted: 13

the radiation extinction coefficient, k_{rad} . k_{rad} ranging from 0.4–0.65 has been measured for coniferous forests and understory shrubs (Wolfe and Thornton, 2011). The NO_x lifetime increased by 2.7% and the canopy fluxes, and above-canopy concentrations decrease by 0.7% and 0.6%, respectively, for a change in k_{rad} from 0 to 0.6 (Fig. S6). This effect is expected to be greater for forests with larger LAI. The minimal effect of k_{rad} on model results was also observed for multiple canopy profile shapes of equivalent LAI.

4 Results

4.1 Model validation: comparison to field observations

To evaluate the applicability of our 1D multilayer canopy model for predicting NO_x concentrations and vertical fluxes in a variety of forest environments, we compared the model to observations from BEARPEX-2009 and UMBS-2012. Parameters used in each calculation are shown in Table 1. The model was run using both the Emberson and Wesely stomatal conductance models. Parameters for temperature, drought stress, and maximum and minimum stomatal conductances used in the Emberson model were input for the dominant tree species in the region (Table 2). At the BEARPEX-2009 site, the dominant tree species was ponderosa pine. For this site, g_{max} and parameters for f_{SWP} and f_{VPD} were inferred from ponderosa pine stomatal conductance data (Kelliher et al., 1995; Ryan et al., 2000; Hubbard et al., 2001; Johnson et al., 2009; Anderegg et al., 2017), and f_{light} was inferred from measurements of the canopy conductance during BEARPEX-2009 (Fig. 3a). f_{temp} was represented by observations for Scots pine (Altimir et al., 2004; Emberson et al., 1997; Buker et al., 2012) and validated with comparison to stomatal conductance measured via sap-flow during BEARPEX-2009 (Fig. 3a). At UMBS the dominant species are quaking aspen and bigtooth aspen, with many birch, beech, and maple species also present (Seok et al., 2013). Data for a European beech tree species was used to represent stomatal conductance parameters (Buker et al., 2007; Buker et al., 2012) and SWP stress (Emberson et al., 2000). These parameters were validated with comparison to stomatal conductance calculated from water vapor and latent heat flux measurements during UMBS-2012 using an energy-balance method according to Mallick et al. (2013) (Fig. 4a).

The model replicates key features of the canopy fluxes and above-canopy NO_x daytime mixing ratios from the 2009 BEARPEX campaign (Fig. 3). The average daytime above-canopy NO_x mixing ratio during the duration of BEARPEX-2009 was 253 ppt, with observations ranging from 80–550 ppt of NO_2 and 10–100 ppt of NO (Min et al., 2014). The general daily trends in observations of NO_x mixing ratios are captured by both the Wesely and Emberson cases—with minimum NO_x mixing ratios occurring in the late morning, an increase of NO_x in the afternoon, and maximum NO_x concentrations of 450–500 ppt reached in the evenings, primarily as a result of high- NO_x plumes from near-by Sacramento in the afternoon (Wolfe et al., 2011; Min et al., 2014) (Fig. 3b). However, both model scenarios predict a slower than observed decrease in NO_x mixing ratios from the evening to the early morning, larger mid-morning fluxes than observed (by $\sim 0.5\text{--}1.5\text{ ppt m s}^{-1}$), and fail to represent the in-canopy enhancement of NO_x ($\sim 50\text{ ppt}$), relative to above-canopy mixing ratios, observed in the evening (Fig. 3). The

Deleted: s

Deleted: is

Deleted: s

Deleted: ere

Deleted: midday

Deleted:

above-canopy vertical NO_x flux predicted in both model cases also agrees reasonably well with observations, with the Emberson case representing morning and midday NO_x fluxes slightly better than the Wesely case. This relatively good agreement between the Emberson case and observed fluxes is also demonstrated in Fig 3d by the agreement between modelled and observed canopy NO_x enhancements. There is, however, generally little difference between Emberson and Wesely model cases for this site during the period considered (Fig 3). This is likely due to the good agreement in both the Emberson and Wesely cases to observations of stomatal conductance (Fig 3a).

We also observe similar correspondence between the model and key features of the UMBS-2012 observations (Fig 4). NO and NO_2 mixing ratios and canopy fluxes are both within the range of observations. The model predicts a maximum of ~40% lower NO_2 in the morning and ~30% higher NO_2 at night than what was observed (Fig 4b). Differences between the Wesely model and Emberson model were negligible for this site. This is likely due to a higher humidity in the summer in this region and larger soil moisture, reducing the prediction for midday and late afternoon VPD stress by the Emberson model, as can be seen by the similarity in the predicted g_s by the Emberson and Wesely models (Fig 4a).

4.2 Effects of maximum stomatal conductance

The BEARPEX-2009 case was simulated using the Wesely model for different values of the maximum stomatal conductance (g_{max}) (Fig 5), with advection concentrations of NO_x set to zero. The range of g_{max} currently represented in the literature during peak growing season for forested regions ranges from 0.2–0.8 cm s^{-1} (Kelliher et al., 1995; Emberson et al., 1997; Emberson et al., 2000; Ryan et al., 2000; Hubbard et al., 2001; Altimir et al., 2003; Fares et al., 2013). This range reflects differences in forest types and a wide variety of tree species. Global CTMs using the Wesely parameterization currently include g_{max} of 1.4, 0.77, and 1 cm s^{-1} for deciduous, coniferous, and mixed forests, respectively (Wesely, 1989; Wang et al., 1998a). Figure 5b demonstrates the impact of g_{max} on the average daily vertical flux of NO_x through the canopy. 96% of soil emitted NO_x is ventilated through the canopy with no foliar deposition ($g_{max}=0 \text{ cm s}^{-1}$). In contrast, 44% of soil-emitted NO_x is taken up by the forest and 56% ventilated through the canopy when the maximum stomatal conductance is 1.4 cm s^{-1} . Figures 5c and 5d show the effects of g_{max} on the diurnal flux through the canopy and the diurnal above canopy NO_x mixing ratio, respectively. Compared with no foliar deposition, a g_{max} of 1.4 cm s^{-1} results in ~60% reduction in the canopy flux and ~50% reduction in the above-canopy NO_x mixing ratio at noon. (Fig. 5c, d). In Figure 6a we show the fraction of soil-emitted NO_x ventilated through the canopy as a function of g_{max} . The model suggests a maximum foliar reduction of NO_x of ~60% for a canopy of 10 m and total LAI of 5.1 m^2/m^2 . Our model also predicts that changes in g_{max} have a greater overall impact on canopy NO_x fluxes at larger leaf resistances and slower foliar uptake. In the range for g_{max} of ~0–0.5 cm s^{-1} , variation in g_{max} can have a large impact on the predicted canopy fluxes of NO_x , which would in turn have a large impact on concentrations and fluxes of O_3 . These values of g_{max} results in deposition velocities in the range expected for most forests, based on laboratory measurements of leaf-level deposition (Hanson and Lindberg, 1991; Rondon and Granat, 1994; Hereid and Monson, 2001; Teklemariam and Sparks, 2006; Pape et al., 2008; Chaparro-Suarez et al., 2011; Breuninger et al., 2013; Delaria et al., 2018) and global analysis suggesting 20–50% reductions in soil-emitted NO_x by vegetation (Jacob and Wofsy, 1990; Yienger and

Deleted: slightly

Deleted:

Deleted: s

Deleted: .

Deleted: max total leaf resistance on

Deleted: (g_{max})

Deleted: This range of

Deleted: is the range

Levy, 1995). Model calculations also predict a strong effect on the lifetimes of NO_x, as shown in Figure 6b, with maximum stomatal conductances of 0.1 cm s⁻¹, 0.3 cm s⁻¹, and 1.4 cm s⁻¹, reducing the NO_x lifetime by ~ 0.7 hrs (~7%), ~1.8 hrs (~18%), and ~3.6 hrs (~36%), respectively, compared with no deposition. Similar trends (not shown) were also observed using parameters for UMBS.

4.3 Emberson model vs. Wesely model comparison

The relative importance of including parameterizations of VPD and SWP in the calculation of stomatal conductance and overall deposition velocity is expected to be regionally variable, along with regional variations in dominant tree species, soil types, and meteorology. We ran the model using BEARPEX-2009 conditions using both the Wesely and Emberson stomatal conductance models under “dry” and “wet” conditions. Under the “dry” scenario the SWP daily minimum and maximum were -2.0 MPa and -1.7 MPa, respectively, with the daily minimum reached at sunset. A minimum daily RH of 40% occurred at noon, with a maximum at midnight of 65%. Summertime is often even drier in regions of the western United States, so these “dry” parameters are conservative estimates for many forests. Under the “wet” scenario the SWP daily minimum and maximum were -0.5 MPa and -0.1 MPa, respectively. The maximum and minimum RH were 90% and 80%, respectively. The values for soil moisture and relative humidity chosen were based on observations of SWP by Ishikawa and Bledose (2000) and the long-term climate data record at Auburn Municipal Airport (38.9547° N, -121.0819° W) from NOAA National Centers for Environmental Information.

The results of the Wesely and Emberson “wet” and “dry” model runs are shown in Figure 8. There was only a slight decrease of the in-canopy NO_x enhancement and of the canopy fluxes in the Wesely “wet” case, presumably due to a slight increase in OH radicals at higher RH. Predictably, the difference in the modelled deposition velocities was quite dramatic between the Emberson “wet” and “dry” cases. In the “dry” scenario, the deposition velocity reached a maximum in the late morning, but rapidly declined after noon. The maximum deposition velocity reached was also substantially reduced (Fig 7a). Using the “wet” Emberson stomatal conductance model, the NO_x flux out of the forest was reduced by 16% midday compared to the “dry” case, and the percent of soil NO_x removed within the canopy was increased from 18% to 30% (Fig 7). The model calculates a substantial impact on above-canopy NO_x mixing ratios (Fig. 8), with a maximum of ~30% difference in NO_x in the afternoon between “wet” and “dry” days using the Emberson parameterizations, compared with ~10% difference using the Wesely model. Using the Emberson parameterization of stomatal conductance, deposition during “wet” days is predicted to contribute substantially more to the total NO_x loss (~40%), with only ~15% contribution predicted for “dry” days (Fig. 9).

Under the Wesely model, where stomatal conductance is parameterized only with temperature and solar radiation, the predicted deposition velocity would be nearly identical between the spring and fall in the western United States and similar semi-arid regions (with comparatively minor temperature effects). While the Emberson model predicts large seasonal differences, the Wesely model fails to account for the dramatic decrease in stomatal conductance seen in the dry seasons in such regions caused by significant reductions in relative humidity and soil water potential (Prior et al., 1997; Panek and Goldstein, 2001; Chaves, 2002; Beedlow et al., 2013). We recognize that the multibox model presented in this work is a

Deleted: a

Deleted: deposition

Deleted: velocity

Deleted:

Deleted: and a deposition velocity of 1.4 cm s⁻¹ reducing the N lifetime by

Deleted:

Deleted:

Deleted:

Deleted: As was demonstrated in our comparison of the model observations from BEARPEX-2009 and UMBS-2012, t

Deleted: of

Deleted:

Deleted: to a minimum shortly

Deleted: is

Deleted:

Deleted: T

Deleted: .

Deleted: T

simplified representation of physical processes, and as such is not likely to (and is not intended to) provide quantitative exactitude for the trends described above. However, we argue for the necessity of incorporating these conceptual advances for accurately representing canopy processes and predicting their effect on the NO_x cycle.

Formatted: Subscript

5 Discussion

5.1 Implications for modelling NO₂ dry deposition

As in our multilayer canopy model, the most common current method of parameterizing stomatal and cuticular deposition in large-scale chemical transport models (CTMs) is through the resistance model framework of Baldocchi (1987). Many global (e.g. WRF-Chem and GEOS-Chem) and regional (e. g. MOZART and CAMx) CTMs calculate the stomatal component of the total deposition resistance using the representation of Wesely (1989), where stomatal conductance is dependent only on the type of vegetation, temperature, and solar radiation. The limitations of this parameterization have been highlighted by observations of a strong dependence of foliar deposition on soil moisture and vapor pressure deficit (VPD) (Kavassalis and Murphy, 2017; Rydsaa et al., 2016). Inadequate descriptions of vegetative species, soil moisture, drought stress, etc., can have a dramatic impact on model results, and result in significant discrepancies between models and observations (Wesely and Hicks, 2000). Failure to account for effects of plant physiology on deposition may result in misrepresentation of deposition velocities, which, as we demonstrate, can have a substantial impact on NO_x lifetimes and mixing ratios above and within a forest canopy. This effect will be especially pronounced in areas, such as much of the western United States, where there are frequent periods of prolonged drought. Parameterizations of stomatal conductance, such as those presented in Emberson et al. (2000) and incorporated into some regional-scale CTMs (e.g. EMEP, MSC-W, and CHIMERE), if incorporated into global atmospheric models, could more accurately reflect the dependence of foliar deposition on meteorology and soil conditions. However, additional laboratory and field measurements on diverse plant species are also needed to determine appropriate, ecosystem-specific inputs to these parameterizations.

It should be noted that there have been significant recent advances in optimization approaches of stomatal modelling based on the theory that stomata maximize CO₂ assimilation per molecule of water vapor lost via transpiration (Medlyn et al., 2011; Bonan et al., 2014; Franks et al., 2017; Miner et al., 2017; Franks et al., 2018). Medlyn et al. (2011) reconciled the empirical widely utilized Ball-Berry model with a theoretical framework optimizing ribulose 1,5 biphosphate (RuBP) regeneration-limited photosynthesis. However, such methods of water use efficiency optimization do not account for stomatal closure as a result of soil moisture stress. Bonan et al. (2014) further developed a model considering water use efficiency optimization and water transport between the soil, plant, and atmosphere. Such parameterizations are utilized in the Community Land Model (CLM)—a land surface model often incorporated into regional and global climate-chemistry models (Lombardozi et al., 2015; Kennedy et al., 2019). Although this model provides a physiological and mechanistic basis for stomatal behaviour, it is heavily parameterized, relying on inputs of plant and soil parameters that could be expected to vary significantly across ecosystem types. For this reason, we view these methods as aspirational for incorporation into atmospheric

global CTMs. We find the relative simplicity of the Emberson approach more useful for the purpose and scope of parameters for large-scale atmospheric models.

Deleted:

5.2 Implications for modelling ozone

~~NO₂~~, as well as O₃, deposition budgets are frequently calculated through inferential methods whereby the deposition velocity is constrained with ambient observations (Holland et al., 2005; Geddes and Murphy, 2014). These inferential models are often complicated by the fast reaction of the NO₂-NO-O₃ triad, making it difficult to separate chemical and physical processes. Further, these inferential models for determining dry deposition constrained with observations of chemical concentrations and eddy covariance measurements of fluxes are difficult to interpret because of similar chemical and turbulent timescales (Min et al., 2014; Geddes and Murphy, 2014). Emission of NO from soils, rapid chemical conversion to NO₂, and subsequent in-air reactions of NO_x must be evaluated accurately in order to correctly infer NO_x and O₃ atmosphere-biosphere exchange from observations. Our multilayer canopy model applies a simple method of representing these processes and evaluating the separate effects of chemistry and dry deposition on the NO_x budget in forests.

Deleted: NO_x

Since the foliar deposition of NO₂ reduces the NO_x lifetime and NO_x that is transported out of the canopy, it will also reduce the amount of ozone that is produced both within and above the canopy. Ozone production efficiency (OPE) in the canopy is calculated using Eq.23-25:

Deleted: 4

$$L(\text{NO}_x) = L_{\text{NO}_x \rightarrow \text{Dep}} + L_{\text{NO}_x \rightarrow \text{RONO}_2} + L_{\text{NO}_x \rightarrow \text{HNO}_3}, \tag{23}$$

Deleted: 6

$$P(\text{O}_3) = k_{\text{HO}_2 + \text{NO}}[\text{HO}_2][\text{NO}] + k_{\text{CH}_3\text{O}_2 + \text{NO}}[\text{CH}_3\text{O}_2][\text{NO}] + (1 - \alpha)k_{\text{RO}_2 + \text{NO}}[\text{RO}_2][\text{NO}], \tag{24}$$

Deleted: 4

$$\text{OPE} = \frac{P(\text{O}_3)}{L(\text{NO}_x)}, \tag{25}$$

Deleted: 5

Deleted: 6

where $P(\text{O}_3)$ is the ozone production rate and $L(\text{NO}_x)$ is the NO_x loss rate. The effect of stomatal conductance to NO₂ on OPE is shown in Figure 6c. An increase in g_{max} from 0 to 0.3 cm s⁻¹ results in a decrease in OPE for the ~~PBL~~ from 24.0 to 20.7 (~14%), and a decrease to 17.0 (~30%) if g_{max} is 1.4 cm s⁻¹. This is similar to OPE calculations that have been reported for forests and environments with NO_x mixing ratios less than 1 ppb and heavily influenced by BVOC emissions (Marion et al., 2001; Browne and Cohen, 2012; Ninneman et al., 2017).

Deleted: planetary boundary layer

~~NO₂~~ deposition and the in-canopy chemistry of NO₂-NO-O₃ also impacts O₃ production and removal. O₃ deposition is frequently inferred from measurements of O₃ concentrations or eddy-covariance measurements (Wesely and Hicks, 2000; Kavassalis and Murphy, 2017). However, because NO₂ has a direct impact on ozone production, deposition of NO₂ can affect inferences of O₃ deposition from observations. The 14% reduction of OPE and more than a 20% reduction in daytime NO_x resulting from an increase in g_{max} from 0 to 0.3 cm s⁻¹ can cause a parallel decrease in O₃ concentrations and fluxes independent from O₃ chemical loss or deposition. Thus, deposition of NO₂ must be taken into account when evaluating O₃ deposition losses from observed canopy fluxes.

Deleted: NO_x

5.3 Implications for near-urban forests

The analysis above suggests that the relative importance of chemical sinks and deposition will vary with NO_x concentration. To evaluate the relative importance of NO₂ foliar deposition and chemistry as a function of NO_x mixing ratio, a simplified 1-box model was also constructed with a simplified reaction scheme (Table S3), VOC reactivity of 8 s⁻¹, α of 0.075, and a HO_x (HO_x ≡ OH + HO₂) production rate (P_{HO_x}) of 2×10⁶ molecules cm⁻³s⁻¹ (similar to conditions observed at BEARPEX-09). RO₂, OH, and HO₂ were solved for steady-state concentrations and NO_x loss pathways were calculated via Eq. 26-29.

$$D_{NO_x} = LAI \cdot V_d \cdot \frac{h_{can}}{h_{PBL}} [NO_2]$$
 (26)

where h_{can} is the canopy height (15m), h_{PBL} is the planetary boundary layer height (1000 m), and LAI is 5 m²/m².

$$P_{HNO_3} = k_{OH+NO_2} [OH] [NO_2]$$
 (27)

$$P_{ANs} = \alpha k_{RO_2+NO} [RO_2] fNO$$
 (28)

where

$$fNO = \frac{k_{RO_2+NO} [NO]}{k_{RO_2+NO} [NO] + k_{RO_2+HO_2} [HO_2] + k_{RO_2+RO_2} [RO_2]}$$
 (29)

The results from this simplified box model are shown in Figure 9 and agree well with our 1D multi-box model near 10 ppb NO_x (Fig S7). With deposition set to zero, nitric acid formation becomes a more significant sink of NO_x than alkyl nitrate formation at around 1 ppb, and nitric acid formation accounts for greater than 70% of the total loss at 100 ppb. With a deposition pathway included, deposition acts as the dominant NO_x sink above 30 ppb and at 10 ppb deposition and AN formation are each 20% of the NO_x sink. Deposition is approximately 10% of the sink over a wide range of concentrations. Forests in close proximity to urban centers (Fig S9) may result in a substantial local decrease in NO_x (Fig S8, Fig 10). Although the influence of urban or near-urban trees on NO_x concentrations would be heavily dependent on meteorological factors (i.e. wind speed and direction), proximity to emission sources, and LAI, it may have some importance on a local or neighborhood scale. This effect may be relevant for understanding and predicting the effects of NO_x reduction policies within and near cities. It may also be useful in considering as a direct nitrogen input to the biosphere, not mediated by soil processes.

6 Conclusions

We have constructed a 1D multi-box model with representations of chemistry and vertical transport to evaluate the impact of leaf-level processes on canopy-scale concentrations, lifetimes, and canopy fluxes of NO_x. Our model is able to closely replicate canopy fluxes and above-canopy NO_x daytime mixing ratios during two field campaigns that took place in a Sierra Nevada pine forest (BEARPEX-2009) and a northern Michigan mixed hardwood forest (UMBS-2012). We conclude that the widely used canopy reduction factor approach to describing soil NO_x removal from the atmosphere within plant canopies is consistent with a process-based model that utilizes stomatal uptake and we recommend that the CRF parameter be replaced with stomatal models for NO₂ uptake.

Deleted: 7

Deleted: 30

Deleted: 7

Deleted: 0.8

Deleted: 8

Deleted: 9

Deleted: 30

Deleted: taking

Deleted: s

Deleted: NO_x

We demonstrate with our 1D multi-box model that NO₂ deposition provides a mechanistic explanation behind canopy reduction factors (CRFs) that are widely used in CTMs. We predict a maximum of ~60% reduction in the fraction of soil-emitted NO_x ventilated through the canopy when stomatal conductances are greater than 0.075 cm s⁻¹, consistent with the range of global CRFs used in current CTMs (Jacob and Wofsy, 1990; Yienger and Levy, 1995). Our model also predicts that changes in g_{max} have a greater overall impact on canopy NO_x fluxes at larger leaf resistances to uptake (slower foliar uptake). In the range for g_{max} of ~0–0.5 cm s⁻¹, errors or variability in stomatal conductance can have a large impact on the predicted canopy concentrations and fluxes of NO_x, which would in turn have large impact on concentrations and fluxes of O₃. This range of deposition velocities describes the range of uptake rates measured for many tree species and forest ecosystems (Hanson and Lindberg, 1991; Rondon and Granat, 1994; Hereid and Monson, 2001; Teklemariam and Sparks, 2006; Pape et al., 2008; Chaparro-Suarez et al., 2011; Delaria et al., 2018). Model calculations also predict a similar trend on the lifetimes of NO_x, with a maximum reduction in the NO_x lifetime by ~4 hrs (>40%) compared with no deposition.

The large effect that small changes in stomatal conductance can have on NO_x lifetimes, concentrations, budget, and O₃ production makes it very important to accurately parameterize in atmospheric models. Most global scale **chemical** transport models parameterize stomatal conductance using **the representation**, developed by Wesely (1989) (Jacob and Wofsy, 1990; Verbeke et al., 2015). These do no account for the effects of VPD, SWP, CO₂ mixing ratio, or other factors known to influence stomatal conductance (Hardacre et al., 2015). We show that incorporating vapor pressure deficit and soil water potential—using the parameterization of Emberson et al. (2000)—has a substantial impact on predicted NO₂ deposition, with the percent of soil NO_x removed within the canopy increasing from 18% to 30% in wet (low VPD and high SWP) conditions compared to dry conditions in the location of BEARPEX-2009. Under the Wesely model, where stomatal conductance is parameterized only with temperature and solar radiation, the predicted deposition velocity would be nearly identical **between “wet” and “dry”** days and between the spring and fall in semi-arid regions (e.g. much of the western United States, **the Mediterranean Basin, the west coast of South America, parts of northwest Africa, parts of western and southern Australia, and parts of South Africa**). The dominant effect of stomatal opening on NO₂ deposition causes an important time of day and seasonal behaviour that should be extensively explored **with observations of NO_x fluxes and concurrent models to confirm the role of deposition in a wider range of environs and more thoroughly vet the conceptual model proposed here**.

Acknowledgements. We wish to gratefully acknowledge financial support from the National Science Foundation (NSF, AGS-1352972). This study was supported by NOAA Climate Program Office’s Atmospheric Chemistry, Carbon Cycle, and Climate program NA18OAR4310117. Additional support was provided by an NSF Graduate Research Fellowship to Erin R. Delaria. We would also like to give a special thanks to Jennifer G. Murphy, University of Toronto and Jeffrey Geddes, Boston University for providing data from the UMBS field site; and J. Geddes for constructive comments that improved the manuscript.

Deleted: chemistry

Deleted: the resistance in-series approach similar to that

Deleted: model

Deleted: Wang and Leuning, 1998; Ganzeveld et al., 2002;

Deleted: .

Deleted: betwee

Deleted: n

Deleted: wet

Deleted: dry

Deleted: .

References

- Altimir, N., Tuovinen, J.-P., Vesala, T., Kulmala, M., Hari, P.: Measurements of ozone removal by Scots pine shoots: calibration of a stomatal uptake model including the non-stomatal component, *Atmospheric Environment*, 38(15), 2387–2398, <https://doi.org/10.1016/j.atmosenv.2003.09.077>, 2004.
- 5 Ammann, M., Ballmoos, P.V., Stalder, M., Suter, M., Brunold, C.: Uptake and assimilation of atmospheric NO₂ — N by spruce needles (*Picea abies*): A field study. *Water, Air, and Soil Pollution*, 85(3), 1497–1502, <https://doi.org/10.1007/BF00477193>, 1995.
- Anderegg, W. R., Wolf, A., Arango-Velez, A., Choat, B., Chmura, D. J., Jansen, S., Kolb, T., Li, S., Meinzer, F., Pita, P., Resco de Dios, V., Sperry, J. S., Wolfe, B. T., and Pacala, S.: Plant water potential improves prediction of empirical stomatal models, *PLoS ONE*, 12, e0185 481f, <https://doi.org/10.1371/journal.pone.0185481>, 2017.
- 10 Baldocchi, D. D., Hicks, B. B., and Camara, P.: A Canopy Stomatal-Resistance Model for Gaseous Deposition to Vegetated Surfaces, *Atmos. Environ.*, 21, 91–101, [https://doi.org/10.1016/0004-6981\(87\)90274-5](https://doi.org/10.1016/0004-6981(87)90274-5), 1987.
- Beedlow, P.A., Lee, E.H., Tingey, D.T., Waschmann, R.S., Burdick, C.A.: The importance of seasonal temperature and moisture patterns on growth of Douglas-fir in western Oregon, USA, *Agr Forest Meteorol*, 169, 174–185, <https://doi.org/10.1016/j.agrformet.2012.10.010>, 2013.
- 15 Bonan, G. B., Williams, M., Fisher, R. A., and Oleson, K. W.: Modelling stomatal conductance in the earth system: linking leaf water-use efficiency and water transport along the soil–plant–atmosphere continuum, *Geosci. Model Dev.*, 7, 2193–2222, <https://doi.org/10.5194/gmd-7-2193-2014>, 2014.
- Breuninger, C., Meixner, F. X., and Kesselmeier, J.: Field investigations of nitrogen dioxide (NO₂) exchange between plants and the atmosphere, *Atmos. Chem. Phys.*, 13, 773–790, <https://doi.org/10.5194/acp-13-773-2013>, 2013.
- 20 Browne, E. C. and Cohen, R. C.: Effects of biogenic nitrate chemistry on the NO_x lifetime in remote continental regions, *Atmos. Chem. Phys.*, 12, 11917–11932, <https://doi.org/10.5194/acp-12-11917-2012>, 2012.
- [Brunet, Y. and Irvine, M. R.: The control of coherent eddies in vegetation canopies: Streamwise structure spacing, canopy shear scale and atmospheric stability, *Bound.-Lay. Meteorol.*, 94, 139–163, 2000.](#)
- 25 [Bryan, A. M., Cheng, S. J., Ashworth, K., Guenther, A. B., Hardiman, B. S., Bohrer, G., and Steiner, A. L.: Forest-atmosphere BVOC exchange in diverse and structurally complex canopies: 1-D modeling of a mid-successional forest in northern Michigan, *Atmos. Environ.*, 120, 217–226, doi:10.1016/j.atmosenv.2015.08.094, 2015.](#)
- Büker, P., Emberson, L.D., Ashmore, M.R., Cambridge, H.M., Jacobs, C.M.J., Massman, W.J., Muller, J., Nikolov, N., Novak, K., Oksanen, E., Schaub, M., and de la Torre, D. Comparison of different stomatal conductance algorithms for ozone flux modelling, *Environmental Pollution*, 146(3), 726–735, <https://doi.org/10.1016/j.envpol.2006.04.007>, 2007.
- 30 Büker, P., Morrissey, T., Briolat, A., Falk, R., Simpson, D., Tuovinen, J.-P., Alonso, R., Barth, S., Baumgarten, M., Grulke, N., Karlsson, P. E., King, J., Lagergren, F., Matyssek, R., Nunn, A., Ogaya, R., Peñuelas, J., Rhea, L., Schaub, M., Uddling, J., Werner, W., and Emberson, L. D.: DO3SE modelling of soil moisture to determine ozone flux to forest trees, *Atmos. Chem. Phys.*, 12, 5537–5562, <https://doi.org/10.5194/acp-12-5537-2012>, 2012.

- Burkholder, J.B., Sander, S.P., Abbatt, J., Barker, J.R., Huie, R.E., Kolb, C. E., Kurylo, M. J., Orkin, V. L., Wilmouth, D. M. and Wine P. H.: Chemical Kinetics and Photochemical Data for Use in Atmospheric Studies, Evaluation No. 18, JPL Publication 15-10, Jet Propulsion Laboratory, Pasadena, <http://jpldataeval.jpl.nasa.gov>, 2015.
- Chaparro-Suarez, I. G., Meixner, F. X., and Kesselmeier, J.: Nitrogen dioxide (NO₂) uptake by vegetation controlled by atmospheric concentrations and plant stomatal aperture, *Atmos. Environ.*, 45, 5742–5750, <https://doi.org/10.1016/j.atmosenv.2011.07.021>, 2011.
- Chaves, M.M.: How Plants Cope with Water Stress in the Field? Photosynthesis and Growth, *Annals of Botany*, 89(7), 907–916, <https://doi.org/10.1093/aob/mcf105>, 2002.
- [Collineau, S. and Brunet, Y.: Detection of turbulent coherent motions in a forest canopy. I. Wavelet analysis, *Bound.-Lay. Meteorol.*, 65, 357–379, 1993.](#)
- Crutzen, P.J.: The Role of NO and NO₂ in the Chemistry of the Troposphere and Stratosphere. *Annual Review of Earth and Planetary Sciences*, 7(1), 443–472, <https://doi.org/10.1146/annurev.ea.07.050179.002303>, 1979.
- Delaria, E. R., Vieira, M., Cremieux, J., and Cohen, R. C.: Measurements of NO and NO₂ exchange between the atmosphere and *Quercus agrifolia*, *Atmos. Chem. Phys.*, 18, 14161–14173, <https://doi.org/10.5194/acp-18-14161-2018>, 2018.
- Emberson, L., Ashmore, M., Cambridge, H., Simpson D., Tuovinen, J.-P.: Modelling stomatal ozone flux across Europe, *Environmental Pollution*, 109(3), 403–413, [https://doi.org/10.1016/S0269-7491\(00\)00043-9](https://doi.org/10.1016/S0269-7491(00)00043-9), 2000.
- Emberson, L.D.: Defining and mapping relative potential sensitivity of European vegetation to ozone. Ph.D. Thesis, Imperial College, University of London, UK, 1997.
- Fares S., Matteucci G., Mugnozza G.S., Morani A., Calfapietra C., Salvatori E., Fursao, L., Manes, F., and Loreto F.: Testing of models of stomatal ozone fluxes with field measurements in a mixed Mediterranean forest. *Atmospheric Environment*, 67, 242–251, <https://doi.org/10.1016/j.atmosenv.2012.11.007>, 2013.
- Fenn M.E., et al. (1998) Nitrogen Excess in North American Ecosystems: Predisposing Factors, Ecosystem Responses, and Management Strategies. *Ecological Applications* 8(3):706.
- [Finnigan, J., Harman, I., Ross, A. and Belcher, S.: First-order turbulence closure for modelling complex canopy flows, *Q. J. R. Meteorol. Soc.*, doi:10.1002/qj.2577, 2015.](#)
- Franks, P.J., Berry, J.A., Lombardozzi, D.L., Bonan, G.B.: Stomatal Function across Temporal and Spatial Scales: Deep-Time Trends, Land-Atmosphere Coupling and Global Models, *Plant Physiology*, 174, 583–602, <https://doi.org/10.1104/pp.17.00287>, 2017.
- Franks, P.J., Bonan, G.B., Berry, J.A., et al.: Comparing optimal and empirical stomatal conductance models for application in Earth system models. *Glob Change Biol.*, 24: 5708– 5723. <https://doi.org/10.1111/gcb.14445>, 2018.
- Galloway, J. N., Dentener, F. J., Capone, D. G., Boyer, E. W., Howarth, R. W., Seitzinger, S. P., Asner, G.P., Cleveland, C.C., Green, P.A., Holland, E.A., Karl, D.M., Michaels, A.F., Porter, J.H., Townsend, A.R., Vörösmarty, C. J.: Nitrogen cycles: Past, present, and future. *Biogeochemistry*, 70(2), 153–226, <https://doi.org/10.1007/s10533-004-0370-0>, 2004.
- Ganzeveld, L. N., Lelieveld, J., Dentener, F. J., Krol, M. C., and Roelofs, G. J.: Atmosphere-biosphere trace gas exchanges simulated with a single-column model, *J. Geophys. Res.-Atmos.*, 107, 4297, <https://doi.org/10.1029/2001jd000684>, 2002.

- Gao W, Wesely ML, Doskey PV (1993) Numerical modelling of the turbulent diffusion and chemistry of NO_x, O₃, isoprene, and other reactive trace gases in and above a forest canopy. *Journal of Geophysical Research: Atmospheres* 98(D10):18339–18353.
- 5 Geddes, J. A. and Murphy, J. G.: Observations of reactive nitrogen oxide fluxes by eddy covariance above two midlatitude North American mixed hardwood forests, *Atmos. Chem. Phys.*, 14, 2939–2957, <https://doi.org/10.5194/acp-14-2939-2014>, 2014.
- Guenther, A., Hewitt, C. N., Erickson, D., Fall, R., Geron, C., Graedel, T., Harley, P., Klinger, L., Lerdau, M. T., McKay, W.A., Pierce, T., Scholes, B., Steinbrecher, R., Tallamraju, R., Taylor, J., and Zimmerman, P.: A global model of natural volatile organic compound emissions, *J. Geophys. Res.*, 100, 8873–8892, <https://doi.org/10.1029/94JD02950>, 1995.
- 10 Gunderson, C. A., Sholtis, J. D., Wullschlegel, S. D., Tissue, D. T., Hanson, P. J. and Norby, R. J.: Environmental and stomatal control of photosynthetic enhancement in the canopy of a sweetgum (*Liquidambar styraciflua* L.) plantation during 3 years of CO₂ enrichment, *Plant, Cell & Environment*, 25, 379–393, <https://doi.org/10.1046/j.0016-8025.2001.00816.x>, 2002.
- Hanson, P. J. and Lindberg, S. E.: Dry Deposition of Reactive Nitrogen-Compounds – a Review of Leaf, Canopy and Non-Foliar Measurements, *Atmos. Environ. A-Gen.*, 25, 1615–1634, [https://doi.org/10.1016/0960-1686\(91\)90020-8](https://doi.org/10.1016/0960-1686(91)90020-8), 1991.
- 15 Hardacre, C., Wild, O., and Emberson, L.: An evaluation of ozone dry deposition in global scale chemistry climate models, *Atmos. Chem. Phys.*, 15, 6419–6436, <https://doi.org/10.5194/acp-15-6419-2015>, 2015.
- Hereid, D. P. and Monson, R. K.: Nitrogen oxide fluxes between corn (*Zea mays* L.) leaves and the atmosphere, *Atmos. Environ.*, 35, 975–983, [https://doi.org/10.1016/S1352-2310\(00\)00342-3](https://doi.org/10.1016/S1352-2310(00)00342-3), 2001.
- Holland, E.A., Braswell, B.H., Lamarque, J.-F., Townsend, A., Sulzman, J., Müller, J.-F., Dentener, F., Brasseur, G., Levy, H.II, Penner, J.E., and Roelofs, G.-J.: Variations in the predicted spatial distribution of atmospheric nitrogen deposition and their impact on carbon uptake by terrestrial ecosystems. *Journal of Geophysical Research: Atmospheres* 102(D13):15849–15866, <https://doi.org/10.1029/96JD03164>, 1997.
- Holland, E.A., Braswell, B.H., Sulzman, J., Lamarque, F.: Nitrogen deposition onto the United States and western Europe: Synthesis of observations and models, *Ecol Appl*, 15, 38–57, <https://doi.org/10.1890/03-5162>, 2005.
- 25 Hubbard, R.M., Ryan, M.G., Stiller, V., and Sperry, J.S.: Stomatal conductance and photosynthesis vary linearly with plant hydraulic conductance in ponderosa pine, *Plant, Cell & Environment*, 24, 113–121, <https://doi.org/10.1046/j.1365-3040.2001.00660.x>, 2001.
- Ishikawa, C.M. and Bledsoe, C.: Seasonal and diurnal patterns of soil water potential in the rhizosphere of blue oaks: evidence for hydraulic lift, *Oecologia*, 125(4), 459–465, <https://doi.org/10.1007/s004420000470>, 2000.
- 30 Jacob D.J. and Wofsy S.C.: Budgets of reactive nitrogen, hydrocarbons, and ozone over the Amazon forest during the wet season. *Journal of Geophysical Research*, 95(D10), 16737, <https://doi.org/10.1029/JD095D10p16737>, 1990.
- Jarvis, P. G., Monteith, J. L., and Weatherley, P. E.: The interpretation of the variations in leaf water potential and stomatal conductance found in canopies in the field. *Phil. Trans. R. Soc. Lond. B*, 273, 593–610, <http://doi.org/10.1098/rstb.1976.0035>, 1976.
- 35 Johansson, C.: Pine forest: a negligible sink for atmospheric NO_x in rural Sweden, *Tellus B*, 39B, 426–438, 1987.

Field Code Changed

- Johnson, D., Woodruff, D., Mcculloh, K., Meinzer, F.: Leaf hydraulic conductance, measured in situ, declines and recovers daily: leaf hydraulics, water potential and stomatal conductance in four temperate and three tropical tree species, *Tree Physiology*, 29(7), 879–887, <https://doi.org/10.1093/treephys/tpp031>, 2009.
- 5 Kavassalis, S.C. and Murphy, J.G.: Understanding ozone-meteorology correlations: A role for dry deposition, *Geophysical Research Letters*, 44(6), 2922–2931, <https://doi.org/10.1002/2016GL071791>, 2017.
- Keilliker, F. F., Leuning, R., Raupach, M.R., and Schulze, E.-D.: Maximum conductances for evaporation from global vegetation types: Agric. For. Meteorol., 73, 1–16, [https://doi.org/10.1016/0168-1923\(94\)02178-M](https://doi.org/10.1016/0168-1923(94)02178-M), 1995.
- 10 [Kennedy, D., Swenson, S., Oleson, K. W., Lawrence, D. M., Fisher, R., Lola da Costa, A. C., and Gentine, P.: Implementing plant hydraulics in the Community Land Model, version 5, *Journal of Advances in Modeling Earth Systems*, 11, 485– 513, <https://doi.org/10.1029/2018MS001500>, 2019.](https://doi.org/10.1029/2018MS001500)
- [Lombardozi, D. L., Bonan, G. B., Smith, N. G., Dukes, J. S., and Fisher, R. A.: Temperature acclimation of photosynthesis and respiration: A key uncertainty in the carbon cycle-climate feedback, *Geophys. Res. Lett.*, 42, 8624–8631, <https://doi.org/10.1002/2015GL065934>, 2015.](https://doi.org/10.1002/2015GL065934)
- 15 Madronich S, Flocke S.: The Role of Solar Radiation in Atmospheric Chemistry. The Handbook of Environmental Chemistry Environmental Photochemistry:1–26, 1999.
- [Makar, P. A., Fuentes, J. D., Wang, D., Staebler, R. M., and Wiebe, H. A.: Chemical processing of biogenic hydrocarbons within and above a temperate deciduous forest, *J. Geophys. Res.*, 104, 3581–3603, 1999.](https://doi.org/10.1175/JHM-D-12-0117.1)
- 20 [Mallick, K., Jarvis, A., Fisher, J.B., Tu, K.P., Boegh, E., and Niyogi, D.: Latent Heat Flux and Canopy Conductance Based on Penman–Monteith, Priestley–Taylor Equation, and Bouchet’s Complementary Hypothesis, *J. Hydrometeor.*, 14, 419–442, <https://doi.org/10.1175/JHM-D-12-0117.1>, 2013.](https://doi.org/10.1175/JHM-D-12-0117.1)
- [Matheny, A. M., Bohrer, G., Garrity, S. R., Howard, C. J., and Vogel, C. S.: Observations of stem water storage in trees of opposing hydraulic strategies, *Ecosphere*, doi:10.1890/ES15-00170.1, 2015.](https://doi.org/10.1890/ES15-00170.1)
- 25 Medlyn, B. E., Duursma, R. A., Eamus, D., Ellsworth, D. S., Prentice, I. C., Barton, C. V., Crous, K. Y., De Angelis, P., Freeman, M. And Wingate, L.: Reconciling the optimal and empirical approaches to modelling stomatal conductance. *Global Change Biology*, 17, 2134–2144, <https://doi.org/10.1111/j.1365-2486.2010.02375.x>, 2011.
- Min, K.-E., Pusede, S. E., Browne, E. C., LaFranchi, B. W., and Cohen, R. C.: Eddy covariance fluxes and vertical concentration gradient measurements of NO and NO₂ over a ponderosa pine ecosystem: observational evidence for within-canopy chemical removal of NO_x, *Atmos. Chem. Phys.*, 14, 5495–5512, <https://doi.org/10.5194/acp-14-5495-2014>, 2014.
- 30 Miner, G. L., Bauerle, W. L., and Baldocchi, D. D.: Estimating the sensitivity of stomatal conductance to photosynthesis: a review. *Plant, Cell & Environment*, 40, 1214– 1238. doi: 10.1111/pce.12871, 2017.
- Nguyen, T.B., Crounse, J.D., Teng, A.P., St. Clair, J.M., Paulot, F., Wolfe, G.M., Wennberg, P.O.: Rapid deposition of oxidized biogenic compounds to a temperate forest, *Proceedings of the National Academy of Sciences*, 112 (5), E392–E401, <https://doi.org/10.1073/pnas.1418702112>, 2015.
- 35 [NOAA: National Centers for Environmental Information, Auburn Municipal Airport: <https://www.ncdc.noaa.gov/cdo-web/datasets/LCD/stations/WBAN:23224/detail>, last access: 07 October, 2019.](https://www.ncdc.noaa.gov/cdo-web/datasets/LCD/stations/WBAN:23224/detail)

- Oren, R., Ellsworth, D.S., Johnsen, K.H., Phillips, N., Ewers, B.E., Maier, C., Schafer, K.V.R., McCarthy, H., Hendrey, G. McNulty, S.G., Katul, G.G.: Soil fertility limits carbon sequestration by forest ecosystems in a CO₂-enriched atmosphere, *Nature*, 411(6836), 469–472, <https://doi.org/10.1038/35078064>, 2001.
- 5 Panek, J.A., Goldstein, A.H.: Response of stomatal conductance to drought in ponderosa pine: implications for carbon and ozone uptake, *Tree Physiology*, 21(5), 337–344, <https://doi.org/10.1093/treephys/21.5.337>, 2001.
- Pape, L., Ammann, C., Nyfeler-Brunner, A., Spirig, C., Hens, K., and Meixner, F. X.: An automated dynamic chamber system for surface exchange measurement of non-reactive and reactive trace gases of grassland ecosystems, *Biogeosciences*, 6, 405–429, <https://doi.org/10.5194/bg-6-405-2009>, 2009.
- 10 Prior, L.D., Eamus, D., Duff, G.A.: Seasonal and Diurnal Patterns of Carbon Assimilation, Stomatal Conductance and Leaf Water Potential in *Eucalyptus tetrodonta* Saplings in a Wet - Dry Savanna in Northern Australia, *Australian Journal of Botany*, 45(2), 241, <https://doi.org/10.1071/BT96017>, 1997.
- [Raupach, M. R., Finnigan, J. J., and Brunet, Y.: Coherent eddies and turbulence in vegetation canopies: The mixing-layer analogy, *Bound.-Lay. Meteorol.*, 78, 351–382, 1996.](#)
- 15 Romer, P. S., Duffey, K. C., Wooldridge, P. J., Allen, H. M., Ayres, B. R., Brown, S. S., Brune, W. H., Crounse, J. D., de Gouw, J., Draper, D. C., Feiner, P. A., Fry, J. L., Goldstein, A. H., Koss, A., Misztal, P. K., Nguyen, T. B., Olson, K., Teng, A. P., Wennberg, P. O., Wild, R. J., Zhang, L., and Cohen, R. C.: The lifetime of nitrogen oxides in an isoprene-dominated forest, *Atmos. Chem. Phys.*, 16, 7623–7637, <https://doi.org/10.5194/acp-16-7623-2016>, 2016.
- Rondon, A. and Granat, L.: Studies on the Dry Deposition of NO₂ to Coniferous Species at Low NO₂ Concentrations, *Tellus B*, 46, 339–352, <https://doi.org/10.1034/j.1600-0889.1994.t014-00001.x>, 1994.
- 20 Ryan, M., Bond, B., Law, B. et al.: Transpiration and whole-tree conductance in ponderosa pine trees of different heights, *Oecologia* 124, 553–560, <https://doi.org/10.1007/s004420000403>, 2000.
- Rydsaa, J., Stordal, F., Gerosa, G., Finco, A., Hodnebrog Ø.: Evaluating stomatal ozone fluxes in WRF-Chem: Comparing ozone uptake in Mediterranean ecosystems, *Atmospheric Environment*, 143, 237–248, <https://doi.org/10.1016/j.atmosenv.2016.08.057>, 2016.
- 25 Seok, B., Helmig, D., Ganzeveld, L., Williams, M. W., and Vogel, C. S.: Dynamics of nitrogen oxides and ozone above and within a mixed hardwood forest in northern Michigan, *Atmos. Chem. Phys.*, 13, 7301–7320, <https://doi.org/10.5194/acp-13-7301-2013>, 2013.
- Simpson, D., Benedictow, A., Berge, H., Bergström, R., Emberson, L. D., Fagerli, H., Flechard, C. R., Hayman, G. D., Gauss, M., Jonson, J. E., Jenkin, M. E., Nyíri, A., Richter, C., Semeena, V. S., Tsyro, S., Tuovinen, J.-P., Valdebenito, Á., and Wind, P.: The EMEP MSC-W chemical transport model – technical description, *Atmos. Chem. Phys.*, 12, 7825–7865, <https://doi.org/10.5194/acp-12-7825-2012>, 2012.
- 30 [Sörgel, M., Trebs, I., Serafimovich, A., Moravek, A., Held, A., and Zetzsch, C.: Simultaneous HONO measurements in and above a forest canopy: influence of turbulent exchange on mixing ratio differences, *Atmos. Chem. Phys.*, 11, 841–855, doi:10.5194/acp-11-841-2011, 2011.](#)
- 35 [Steiner, A. L., Pressley, S. N., Botros, A., Jones, E., Chung, S. H., and Edburg, S. L.: Analysis of coherent structures and atmosphere-canopy coupling strength during the CABINEX field campaign, *Atmos. Chem. Phys.*, 11, 11921–11936, doi:10.5194/acp-11-11921-2011, 2011.](#)

- Stern, M.A., Anderson, F.A., Flint, L.E., Flint, A.L.: Soil moisture datasets at five sites in the central Sierra Nevada and northern Coast Ranges, California. Data Series, <https://doi.org/10.3133/ds1083>, 2018.
- Stroud, C., Makar, P., Karl, T., Guenther, A., Geron, C., Turnipseed, A. A., Nemitz, E., Baker, B., Potosnak, M., and Fuentes, J. D.: Role of canopy-scale photochemistry in modifying biogenicatmosphere exchange of reactive terpenoid species: Results from the CELTIC field study, *J. Geophys. Res.*, **110**, D17303, doi:10.1029/2005JD005775, 2005.
- Teklemariam, T. A. and Sparks, J. P.: Leaf fluxes of NO and NO₂ in four herbaceous plant species: The role of ascorbic acid, *Atmos. Environ.*, **40**, 2235–2244, <https://doi.org/10.1016/j.atmosenv.2005.12.010>, 2006.
- Thoene, B., Schroder, P., Papen, H., Egger, A., and Rennenberg, H.: Absorption of Atmospheric NO₂ by Spruce (*Picea-Abies* L Karst) Trees 1, NO₂ Influx and Its Correlation with Nitrate Reduction, *New Phytol.*, **117**, 575–585, <https://doi.org/10.1111/j.1469-8137.1991.tb00962.x>, 1991.
- Thomas, C. and Foken, T.: Flux contribution of coherent structures and its implications for the exchange of energy and matter in a tall spruce canopy, *Bound.-Lay. Meteorol.*, **123**, 317–337, 2007.
- Townsend A.R., Braswell B.H., Holland E.A., and Penner J.E.: Spatial and Temporal Patterns in Terrestrial Carbon Storage Due to Deposition of Fossil Fuel Nitrogen. *Ecological Applications*, **6**(3), 806–814, <https://doi.org/10.2307/2269486>, 1996.
- Verbeke, T., Lathièrre, J., Szopa, S., and de Noblet-Ducoudré, N.: Impact of future land-cover changes on HNO₃ and O₃ surface dry deposition, *Atmos. Chem. Phys.*, **15**, 13555–13568, <https://doi.org/10.5194/acp-15-13555-2015>, 2015.
- Vinken, G. C. M., Boersma, K. F., Maasakkers, J. D., Adon, M., and Martin, R. V.: Worldwide biogenic soil NO_x emissions inferred from OMI NO₂ observations, *Atmos. Chem. Phys.*, **14**, 10363–10381, <https://doi.org/10.5194/acp-14-10363-2014>, 2014.
- Vitousek, P. M., Aber, J. D., Howarth, R. W., Likens, G. E., Matson, P. A., Schindler, D. W., Schlesinger, W. H. and Tilman, D. G.: Human Alteration of the Global Nitrogen Cycle: Sources and Consequences, *Ecological Applications*, **7**(3), 737–750, [https://doi.org/10.1890/1051-0761\(1997\)007\[0737:HAOTGN\]2.0.CO;2](https://doi.org/10.1890/1051-0761(1997)007[0737:HAOTGN]2.0.CO;2), 1997.
- Wang, Y., Jacob D.J., and Logan, J.A.: Global simulation of tropospheric O₃-NO_x-hydrocarbon chemistry: 1. Model formulation, *Journal of Geophysical Research: Atmospheres*, **103**(D9), 10713–10725, <https://doi.org/10.1029/98JD00158>, 1998a.
- Wang, Y., Logan, J.A., Jacob D.J.: Global simulation of tropospheric O₃-NO_x-hydrocarbon chemistry: 2. Model evaluation and global ozone budget, *Journal of Geophysical Research: Atmospheres*, **103**(D9), 10727–10755, <https://doi.org/10.1029/98JD00157>, 1998b.
- Wang, Y.-P. and Leuning, R.: A two-leaf model for canopy conductance, photosynthesis and partitioning of available energy I, *Agricultural and Forest Meteorology*, **91**(1-2), 89–111, [https://doi.org/10.1016/S0168-1923\(98\)00061-6](https://doi.org/10.1016/S0168-1923(98)00061-6), 1998.
- Wesely, M. L. and Hicks, B. B.: A review of the current status of knowledge on dry deposition, *Atmos. Environ.*, **34**, 2261–2282, 2000.
- Wesely, M.: Parameterization of surface resistances to gaseous dry deposition in regional-scale numerical models, *Atmospheric Environment*, **23**(6), 1293–1304, [https://doi.org/10.1016/0004-6981\(89\)90153-4](https://doi.org/10.1016/0004-6981(89)90153-4), 1989.
- Wild, O.: Modelling the global tropospheric ozone budget: exploring the variability in current models, *Atmos. Chem. Phys.*, **7**, 2643–2660, <https://doi.org/10.5194/acp-7-2643-2007>, 2007.

Deleted: 1

- Williams, M. , Rastetter, E. B., Fernandes, D. N., Goulden, M. L., Wofsy, S. C., Shaver, G. R., Melillo, J. M., Munger, J. W., Fan, S. And Nadelhoffer, K. J.: Modelling the soil-plant-atmosphere continuum in a Quercus-Acer stand at Harvard Forest: the regulation of stomatal conductance by light, nitrogen and soil/plant hydraulic properties. *Plant, Cell and Environment* 19(8):911–927, <https://doi.org/10.1111/j.1365-3040.1996.tb00456.x>, 1996.
- 5 Wolfe, G. M. and Thornton, J. A.: The Chemistry of Atmosphere-Forest Exchange (CAFE) Model – Part 1: Model description and characterization, *Atmos. Chem. Phys.*, 11, 77–101, <https://doi.org/10.5194/acp-11-77-2011>, 2011.
- 10 Wolfe, G. M., Thornton, J. A., Bouvier-Brown, N. C., Goldstein, A. H., Park, J.-H., McKay, M., Matross, D. M., Mao, J., Brune, W. H., LaFranchi, B. W., Browne, E. C., Min, K.-E., Wooldridge, P. J., Cohen, R. C., Crounse, J. D., Faloona, I. C., Gilman, J. B., Kuster, W. C., de Gouw, J. A., Huisman, A., and Keutsch, F. N.: The Chemistry of Atmosphere-Forest Exchange (CAFE) Model – Part 2: Application to BEARPEX-2007 observations, *Atmos. Chem. Phys.*, 11, 1269–1294, <https://doi.org/10.5194/acp-11-1269-2011>, 2011.
- [Yi, C.: Momentum Transfer within Canopies, *J. Appl. Meteorol. Clim.* 47, 262–275, doi:10.1175/2007JAMC1667.1, 2008.](#)
- Yienger, J.J. and Levy, H.: Empirical model of global soil-biogenic NO_x emissions, *Journal of Geophysical Research*, 100(D6), 11447–11464, <https://doi.org/10.1029/95JD00370>, 1995.
- 15 Zhang, L., Padro, J., Walmsley, J.: A multi-layer model vs single-layer models and observed O₃ dry deposition velocities, *Atmospheric Environment*, 30(2), 339–345, [https://doi.org/10.1016/1352-2310\(95\)00286-8](https://doi.org/10.1016/1352-2310(95)00286-8), 1996.
- [Zhang, L., Moran, M., Makar, P., Brook, J., and Gong, S.: Modelling Gaseous Dry Deposition in AURAMS A Unified Regional Air-quality Modelling System, *Atmos. Environ.*, 36, 537–560, 2002.](#)
- 20 [Zhang, L., Brook, J. R., and Vet, R.: A revised parameterization for gaseous dry deposition in air-quality models, *Atmos. Chem. Phys.*, 3, 2067–2082, https://doi.org/10.5194/acp-3-2067-2003, 2003.](#)

Table 1: Parameters used in the model for comparison to observations from UMBS and BEARPEX-2009

Parameter	Symbol	UMBS	BEARPEX
Canopy height	h_{can}	^a 20 m	^b 10 m
Understory height	h_{us}	^c 4 m	^b 2 m
Total leaf area index	LAI	^d3.5 m ² /m ²	^b 5.1 m ² /m ²
Radiation extinction coefficient	k_{rad}	^a0.4	^a0.4
Diffusion timescale ratio	τ/T	^a2	^a2
Friction velocity	u^*	^a61 cm s ⁻¹	^a61 cm s ⁻¹
Maximum NO emission flux	eNO_{max}	^a0.7 ppt ms ⁻¹	^b 3 ppt ms ⁻¹
Minimum NO emission flux	eNO_{min}	^a0.3 ppt ms ⁻¹	^b 1 ppt ms ⁻¹
VOC basal emission flux	E_b	^d5 ppb m s ⁻¹	^b 11 ppb m s ⁻¹
Integration interval	Δt	2	2
OH + VOC rate constant (cm ³ molecules ⁻¹ s ⁻¹)	k_{OH}	^e9.8 × 10 ⁻¹¹	^e8.7 × 10 ⁻¹¹
NO ₃ + VOC rate constant (cm ³ molecules ⁻¹ s ⁻¹)	k_{NO_3}	^e7.0 × 10 ⁻¹³	^e1.7 × 10 ⁻¹⁴
Minimum daily temperature		15 °C	17 °C
Maximum daily temperature		23 °C	27 °C
Maximum daily relative humidity		85%	65%
Minimum daily relative humidity		65%	30%
Maximum daily soil water potential		^f-0.05 MPa	^f-0.8 MPa
Minimum daily soil water potential		^f-0.25 MPa	^f-1.0 MPa

a. [Geddes and Murphy, 2014.](#)
b. [Wolfe and Thornton, 2011.](#)
c. [Seok et al., 2013](#)
d. [estimated from Bryan et al., 2015.](#)
e. [See text, calculated assuming dominant VOC is MBO for Blodgett and isoprene for UMBS](#)
f. [Estimated from Matheny et al., 2015.](#)
g. [Taken from Ishikawa and Bledsoe \(2000\) and Stern et al. \(2018\)](#)

Deleted: ^a

Deleted: ^a

Deleted: ^a

Deleted: ⁰

Deleted: ^a

Formatted: Superscript

Formatted: Superscript

Formatted: Font: 8 pt

Formatted: Left, Line spacing: single, Numbered + Level + Numbering Style: a, b, c, ... + Start at: 1 + Alignment: L + Aligned at: 0.25" + Indent at: 0.5"

Deleted: <#>¶

Formatted: Font: 9 pt

Formatted: Font: 8 pt

Formatted: Font: 8 pt

Formatted: Font: 8 pt

Formatted: Font: 8 pt

Formatted: Font: 8 pt

Formatted: Font: 8 pt

Formatted: Left, Indent: Left: 0.5", Line spacing: single, No bullets or numbering

Table 2: Parameters used in the Emberson model for stomatal conductance

	UMBS	reference	BEARPEX	reference
g_{\max} (cm s ⁻¹)	0.2	Büker et al. 2012	0.3	Altimir et al. 2003
f_{\min}	0.05	Büker et al. 2012	0.03	Büker et al. 2012
$Light_a$	0.001	Büker et al. 2012	0.001	This study
T_{\max} (°C)	33	Büker et al. 2012	35	Altimir et al. 2003
T_{\min} (°C)	5	Büker et al. 2012	5	Altimir et al. 2003
T_{opt} (°C)	16	Büker et al. 2012	20	Altimir et al. 2003
VPD_{\min} (kPa)	3.1	Büker et al. 2012	4	Ryan et al. 2000, Hubbard et al. 2001, Kolb and Stone 1999
VPD_{\max} (kPa)	1.1	Büker et al. 2012	1.5	Ryan et al. 2000, Hubbard et al. 2001, Kolb and Stone 1999
SWP_{\max} (MPa)	-1.0	Emberson et al. 2000	-1.0	Anderegg et al. 2017
SWP_{\min} (MPa)	-1.9	Emberson et al. 2000	-2.0	Anderegg et al. 2017

Figures

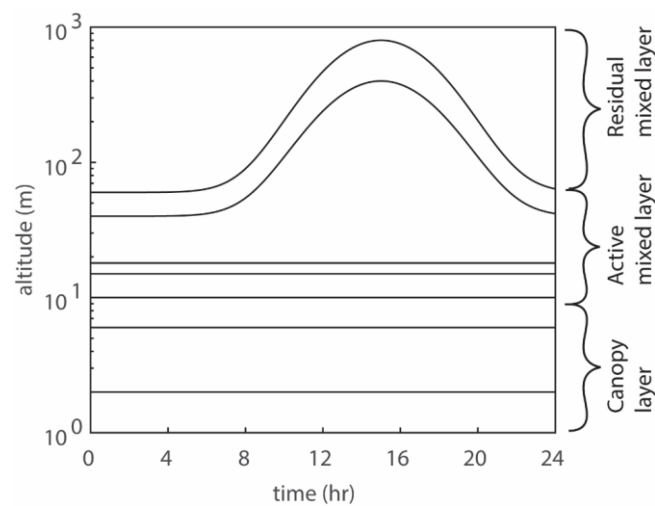


Figure 1: Planetary boundary dynamics in the 1D multibox model. The model domain consists of three boxes in the canopy layer, four in the active mixed layer, and one in the residual mixed layer. The lower five boxes have fixed heights, while the sixth and seventh boxes evolve throughout the day, in the form of a Gaussian function.

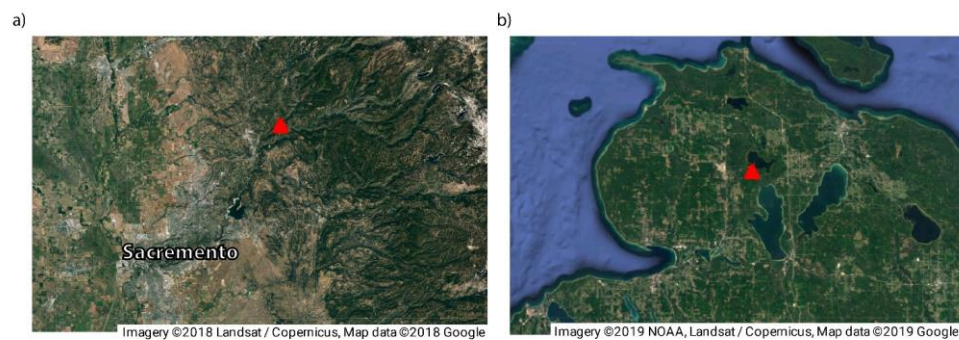


Figure 2: Satellite images showing the locations of (a) the BEARPEX-2009 campaign and (b) the University of Michigan Biological Station (UMBS). Red triangles show the specific site locations. Measurements of chemical species and local meteorological variables from the two campaigns were used to validate our 1D canopy multibox model.

Deleted: <object><object><object>

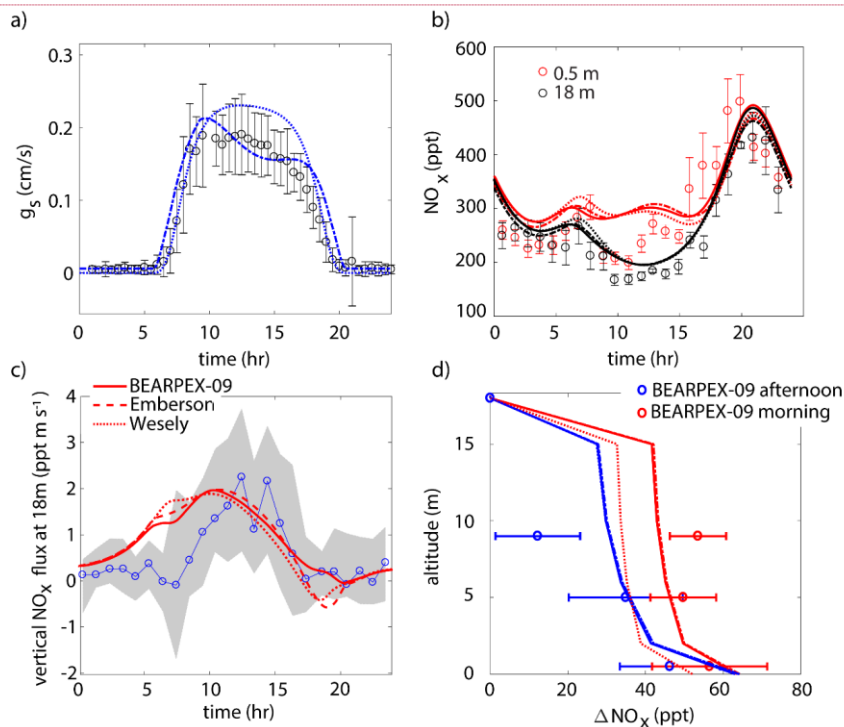


Figure 3: Comparison of model results to BEARPEX-2009 hourly averaged observations of (a) stomatal conductances, (b) NO_x mixing ratios at 18 m (black) and 0.5 m (red) and (c) vertical fluxes at 18 m. (d) Averaged observations of in-canopy NO_x enhancements from 09:00–12:00 (blue) and 13:00–16:00 (red) compared with modeled NO_x enhancements, defined as the difference between NO_x below the canopy and NO_x measured at 18 m. Observations from BEARPEX-2009 are from Min et al., (2014). In all panels solid lines, dotted lines, and dashed lines, represent results from our model with stomatal conductances parameterized using observed conductances, the Wesely model, and the Emberson model, respectively. Circles, error bars, and grey shaded regions represent observations, standard errors of the mean, and the interquartile range of data, respectively.

Deleted: <object>

Deleted: (a) Comparison of 1-hr mean averages of observed stomatal conductances during BEARPEX-2009 (black circles) and stomatal conductances modeled using the Wesely (dotted blue) and Emberson (dashed blue) schemes for June 30, 2009.

Deleted: from observations (circles) and modeled using observed stomatal conductances (solid lines) and the Wesely (dotted lines) and Emberson (dashed lines) parameterizations. (c) Observations of vertical fluxes (blue circles) and fluxes modeled using observed stomatal conductances (solid line) or Wesely (dotted line) and Emberson (dashed line) parameterizations. The grey shaded area gives the interquartile range of the observed flux data for hourly bins.

Deleted: (circles) in the morning

Deleted: afternoon

Deleted:

Deleted: using measured canopy conductances (solid lines), and the Wesely (dotted lines) and Emberson (dashed lines) scenarios...

Deleted: Error bars represent standard errors of the mean.

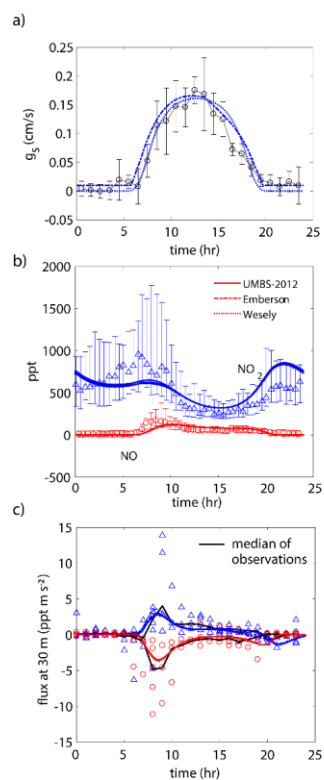


Figure 4: Comparison of model results to (a) hourly averaged observed stomatal conductances, (b) NO and NO₂ mixing ratios at 30 m, and (c) median (black lines) and hourly-averaged NO and NO₂ vertical fluxes at 30 m observed during UMBS-2012 for August 8, 2012. In all panels solid lines, dotted lines, and dashed lines, represent results from our model with stomatal conductances parameterized using observed conductances, the Wesely model, and the Emberson model, respectively. Blue triangles and red circles represent NO₂ and NO observations, respectively. Error bars represent the interquartile range of data.

Deleted: <object>

Deleted: (a) Comparison of averaged observed stomatal conductances at UMBS-2012 (black circles) and modeled stomatal conductances using the Wesely (dotted line) and Emberson (dashed line) scenarios for August 8, 2012. Error bars represent standard deviations of 1-hr averaged values. (b) Observations of NO (red circles) and NO₂ (blue triangles) mixing ratios at 30 m during UMBS-2012 and modeled NO (red) and NO₂ (blue) mixing ratios using measured stomatal conductances (solid lines) and the Wesely (dotted lines) and Emberson (dashed lines) parameterizations. Error bars give the interquartile range of flux data. (c) Median (black lines) and hourly-averaged NO (red circles) and NO₂ (blue triangles) observed vertical fluxes at 30 m compared to modeled NO (red) and NO₂ (blue) fluxes using measured stomatal conductances (solid lines) and the Wesely (dotted lines) and Emberson (dashed lines) parameterizations. ...

Formatted: Subscript

Formatted: Subscript

Formatted: Subscript

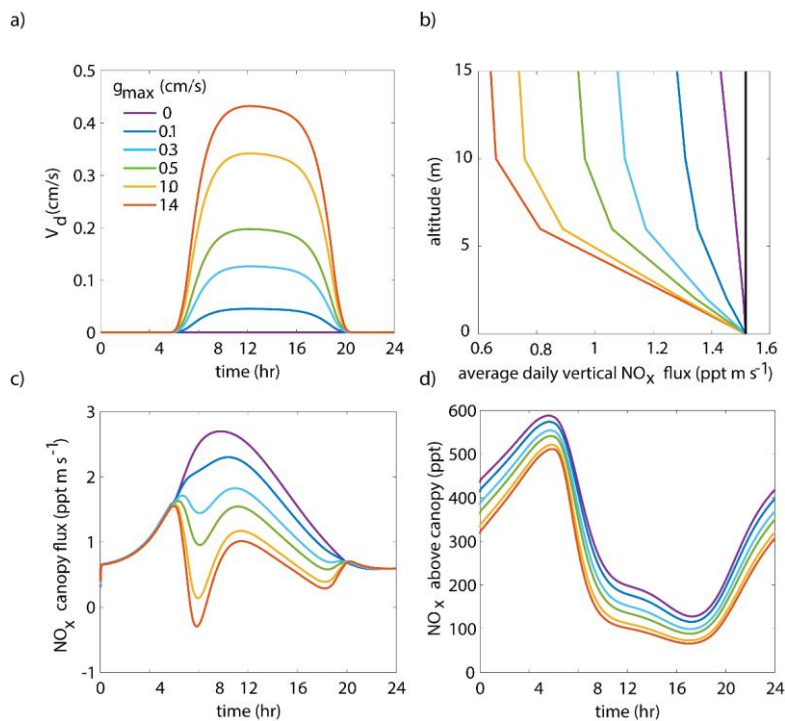


Figure 5: Model results of (a) diurnal NO_2 deposition velocities, (b) average daily vertical fluxes of NO_x and a conserved tracer (black line), (c) diurnal canopy fluxes at 10 m, and (d) diurnal above-canopy NO_x mixing ratios at 15 m for different values of maximum stomatal conductance (g_{max}) using the Wesely scheme to calculate stomatal conductance.

Deleted: Remnant

Deleted: Modeled d

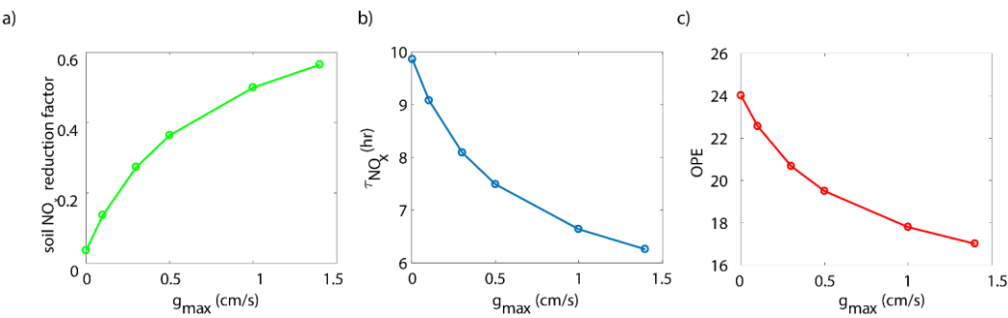
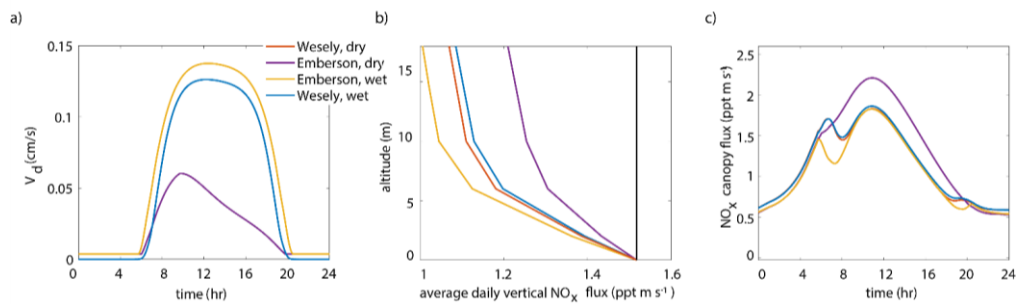


Figure 6: Model-predicted dependence of (a) ~~the fraction of soil emitted~~ NO_x ~~removed in the canopy~~, (b) the average daily NO_x lifetime (τ_{NO_x}) in the planetary boundary layer, and (c) ozone production efficiency (OPE) on maximum stomatal conductance (g_{max}) using the Wesely scheme to calculate stomatal conductance.

Deleted: the percent of soil-emitted
Deleted: removed within the canopy

5



Deleted:

10

Figure 7: Modeled results of (a) diurnal NO₂ deposition velocities, (b) average daily vertical fluxes compared to a conserved tracer (black line), and (c) diurnal canopy fluxes at 10 m for “wet” and “dry” scenarios using either the Wesely or Emberson models to calculate stomatal conductance.

Deleted: Modeled

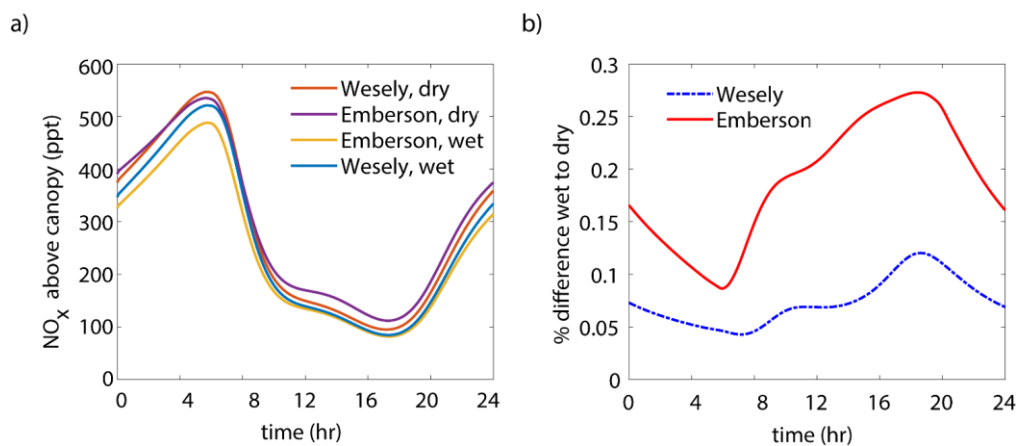
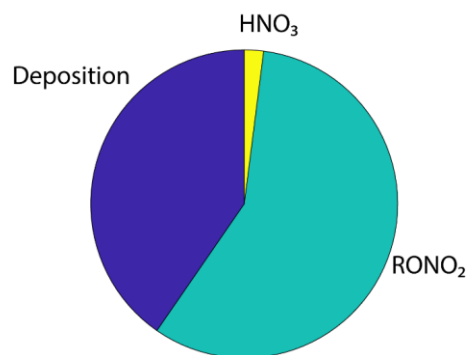


Figure 8: (a) Modeled NO_x mixing ratios above the canopy at 18 m for “wet” and “dry” scenarios using either the Wesely or Emberson models to calculate stomatal conductance. (b) Percent difference between NO_x mixing ratios on “wet” and “dry” days using either the Wesely (blue dashed line) or Emberson (red solid line) parameterization of stomatal conductance.

5

a)



b)

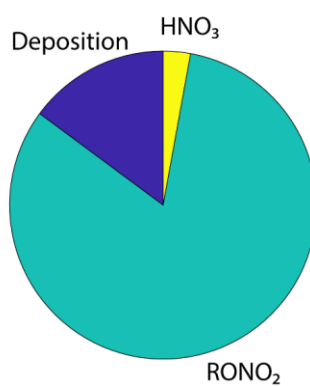


Figure 9: Model prediction for the daytime average fraction of NO_x removed by deposition, nitric acid formation, and alkyl nitrate formation using the Emberson parameterization of stomatal conductance for (a) “wet” and (b) “dry” conditions.

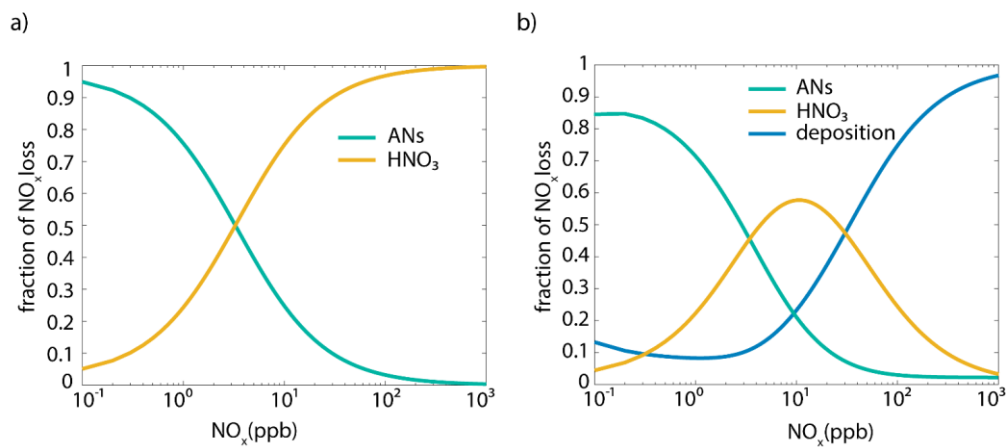


Figure 10: Fraction of NO_x loss to alkyl nitrate formation (green line), nitric acid formation (yellow line) with (a) no foliar uptake and (b) with foliar deposition (blue line) as a function of NO_x mixing ratio predicted by the simplified single-box model.